Analysis of Toxin-Antitoxin System

in *Thermus thermophilus* HB27

A Dissertation Submitted to
the Graduate School of Life and Environmental Sciences,
the University of Tsukuba
in Partial Fulfillment of the Requirements
for the Degree of Doctor of Philosophy
(Doctoral Program in Integrative Environment and Biomass Sciences)

Yuqi Fan

ABREVIATIONS

Dox : doxycycline

DTT : dithiothreitol

IPTG : isopropyl-β-D-thiogalactopyranoside

PAGE : polyacrylamide gel electrophoresis

PBS : phosphate-buffered saline

PMSF : Phenylmethanesulfonylfluoride

RNase : ribonuclease

TA : toxin-antitoxin

TABLE OF CONTENTS

ABREVIATIONS i

ABSTRACT v

LIST OF TABLES ix

LIST OF FIGURES x

CHAPTER I - INTRODUCTION 1

Section I - Thermophiles and Evolution of Life 1

1-1-1 Ancestral life 1

1-1-2 Thermophiles 2

Section II - *Thermus thermophilus* 4

1-2-1 The phylum *Deinococcus-Thermus* 4

1-2-2 *Thermus thermophilus* 4

Section III - Toxin-Antitoxin System 6

1-3-1 Toxin-antitoxin system 6

1-3-2 Types of toxin-antitoxin system 7

CHAPTER II – IDENTIFICATION OF PUTATIVE TOXIN-ANTITOXIN SYSTEMS IN *THERMUS THERMOPHILUS* HB27 9

Section I - Introduction 9

Section II - Materials and Methods 11

2-2-1 Bacterial strains, plasmids and media 11

2-2-2 Plasmid construction 11

2-2-3 Alignment and phylogenetic analysis 11

2-2-4 Growth inhibition assay 12

Section III - Result 15

2-3-1 Analysis of TA locus in *T. thermophilus* 15

2-3-2 Phylogenetic analysis 15

2-3-2 Identification of TA systems using toxin-mediated growth inhibition assays 16

Section IV - Discussion 22
CHAPTER III – IDENTIFICATION OF ENZYME ACTIVITY 24
OF TTC0125-TTC0126 LOCUS 24
Section I – Introduction 24
Section II - Materials and methods 25
3-2-1 Bacterial strains, plasmids and media 25
3-2-2 Plasmid construction 25
3-2-3 Purification of TTC0125 and TTC0126 26
3-2-4 RNA degradation assay 27
3-2-5 *in vitro* translation inhibiton assay 28
Section III – Result 31
3-3-1 Purification of TTC0125 and TTC0126 31
3-3-2 TTC0125 degrades free rRNA and mRNA 31
3-3-3 TTC0125 not degrade tRNA or rRNA in intact ribosome 32
3-3-5 TTC0125 inhibits translation by degrading mRNA 33
Section IV - Discussion 39
CHAPTER IV – IDENTIFICATION OF CATALYTICALLY-IMPORTANT RESIDUES OF TTC0125 42
Section I - Introduction 42
Section II - Materials and methods 43
4-2-1 Bacterial strains, plasmids and media 43
4-2-2 Site-directed mutagenesis 43
4-2-3 Growth inhibition assay 43
4-2-4 RNA degradation assay 44
Section III – Result 46
4-3-1 Conserved amino acid residues of VapCs 46
4-3-2 Growth inhibition assay of TTC0125 mutants. 46
4-3-3 Three-dimensional model of TTC0125 47
4-3-4 Purification of mutants. 48

4-3-5 RNase assay of mutants. 48
Section IV – Discussion 55
CHAPTER V – PHYSIOLOGICAL ANALYSES OF TTC0125-TTC0126 TA LOCUS 58
Section I - Introduction 58
Section II - Materials and methods 61
5-2-1 Bacterial strains, plasmids and media 61
5-2-2 Disruption of TTC0125 gene and TTC0125-TTC0126 locus 61
5-2-3 Reverse transcriptase PCR 62
5-2-4 Minimal Inhibitory Concentration (MIC) against antibiotics 63
5-2-5 Biochemical Assays and Stress Experiments 63
Section III - Result 67
5-3-1 Disruption of TTC0125/TTC0125-TTC0126 changed cell response to kanamycin 67
5-3-2 TTC0125-TTC0126 locus is included in Metabolic-related operon 68
Section IV - Discussion 73
CONCLUSION 76
AKNOWLEDGEMENTS 81
REFERENCES 83

ABSTRACT

Toxin-antitoxin (TA) loci are widely distributed in chromosomes and plasmids of *Bacteria* and *Archaea*. Chromosomes of some of these bacteria contain several TA loci, especially in one of the *Mycobacterium* species, *M. tuberculosis*, which possesses the largest number of putative TA loci on its chromosome, accounting for 79 loci. TA systems consist of two small genes that encode a low molecular weight toxic protein (toxin) which reacts with intracellular target molecules related to essential cellular processes, such as DNA replication, protein translation, membrane integrity, and cell wall synthesis, and a cognate antitoxin protein or RNA that inhibits toxin activity. Initially, TA loci were reported to play a role in bacterial programmed cell death for maintaining plasmid stability by killing the daughter cells that failed to inherit the plasmids, or for acting as antiviral factors. More recently, it was recognized that the toxins play roles in response to cellular stresses, such as amino acid starvation and the presence of antibiotics, and triggering bacterial persistence. Currently, TA systems are grouped into six classes according to the mechanisms used by the antitoxins to neutralize the activities of the toxins. Type II toxin-antitoxin (TA) loci are characterized by encoding two proteins, a stable toxin and an unstable antitoxin which neutralizes the toxin activity by forming a protein complex. In stress conditions, the unstable antitoxin protein is promptly degraded via proteolysis so that the toxin is released from protein complex and becomes active to react with intracellular target molecules, such as mRNA at the ribosomal A site, initiator $tRNA^{fMet}$, Sarcin-Ricin loop of 23S rRNA or glutamyl-tRNA synthetase and EF-Tu proteins, to inhibit cell growth or finally lead to cell death. TA systems are not redundant, as each system may have developed to

respond to specific stresses. Understanding of the detailed chemical and physiological functions of toxins is important for interpretation of their roles in bacterial physiology.

Despite many studies on mesophilic bacteria, including pathogens, the mechanisms and roles of TA systems in thermophilic microorganisms remain unknown. Based on the toxin-antitoxin database, 12 TA loci are predicted to be present in the *Thermus thermophilus* HB27 genome, of which seven are classified into known type II TA families, three (TTC1395-TTC1394, TTC1549-TTC1548, and TTC1705-TTC1704) in HicAB family and four (TTC0113-TTC0114, TTC0125-TTC0126, TTC1207-TTC1208, and TTC1804-TTC1805) in VapBC family. However, experimental analyses on these TA loci have not yet been reported. Here, I analyzed genetically these seven loci, and detailed biochemical analyses of TTC0125-TTC0126 were conducted.

Similarity searches of seven putative toxins in *T. thermophilus* genome with the validated toxins in the Uniprot database indicated low-to-moderate similarities. TTC0113, TTC0125, TTC1207, and TTC1804 showed 24, 44, 12, and 13 % similarity to VapC of *Mycobacterium smegmatis* (VAPC_MYCS2), and TTC1395, TTC1549 and TTC1705 showed 37, 13 and 42 % similarity to HicA of *Escherichia coli*, respectively. Expression of these putative toxin genes in *E. coli* showed that one VapC toxin TTC0125 and two HicA toxins TTC1395 and TTC1705 inhibited cell growth, especially at 43 °C, and co-expression with their cognate antiotoxin genes rescued the growth, indicating that these genes actually function as TA.

VapC family proteins contain a PIN domain and function as RNases. In order

to assess the molecular function of VapC in *T. thermophilus*, I purified protein of VapC toxin TTC0125 and its cognate VapB antitoxin TTC0126 for biochemical analysis, and RNase assays were conducted using total RNA isolated from both *E. coli* and *T. thermophilus*, and an *in vitro*-transcribed mRNA as substrates. The results showed that TTC0125 has an RNase activity to rRNA and mRNA, and this activity was inhibited by addition of the antitoxin TTC0126. Moreover, TTC0125 does not possess substrate- or sequence-specificity, rather it degrades free RNA. Translation inhibition assays showed that TTC0125 inhibited protein synthesis by degrading mRNA but not by inactivation of ribosome via degradation of rRNA in intact ribosomes. Second, I conducted site-directed mutagenesis to identify catalytically-important residues of TTC0125. The result of growth inhibition assay and *in vitro* RNase assay, using purified mutant proteins, showed that 9 residues, D4, E40, A76, G94, G98, D99, S102, D119, and D124, are important for the toxin activity of TTC0125. A three-dimensional model of TTC0125, constructed by the Phyre2 program, indicated that most of the residues, except for G94 and D124, are putative catalytic residues or located around the putative catalytic center, suggesting that these residues are involved in catalysis, substrate binding or structural maintenance of the catalytic center.

RT-PCR analyses showed that TTC0125-TTC126 locus is included in a gene cluster encoding metabolic enzymes related to the glyoxylate and malate synthesis, which is distinct from most *vapBC* loci in microorganisms consisting of a bicystronic operon. Disruption of TTC0125 or TTC0125-TTC0126 locus increased resistance to low dose of kanamycin. This result is different from other reported VapCs, whose disruption reduce survival upon stress condition, indicating TTC0125-TTC126 has a

novel physiological function, which may be related to the glyoxylate cycle.

Keywords: *Thermus thermophilus*; toxin-antitoxin; VapBC; HicBA; glyoxylate-malate metabolism

LIST OF TABLES

Table 2-2-1 TM medium.....13

Table 2-2-2 Primers used in this chapter 14

Table 2-3-1 Toxin-antitoxin genes in *T. thermophilus* HB27 17

Table 3-2-1 Primers used in this chapter 30

Table 4-2-1 Primers used in this chapter 45

Table 5-2-1 Primers used in this chapter 65

Table 5-2-2 MM medium 66

LIST OF FIGURES

Figure 1-1-1 Universal phylogenetic tree determined from rRNA sequence comparisons 3

Figure 2-3-1 Phylogenetic relationships of toxin genes from *Bacteria* and *Archaea* ...18

Figure 2-3-2 Growth inhibition assay..... 20

Figure 2-3-3 Growth inhibition test triggered by induction of TTC0125 (a) or TTC0125-TTC0126 (b) at 37 ºC 21

Figure 3-3-1 SDS-PAGE of the purified TTC0125 and TTC0126 proteins.....34

Figure 3-3-2 RNA degradation assay 35

Figure 3-3-3 RNA degradation assay with intact ribosomes from *E. coli* (a) and *T. thermophilus* (b), and with initiator tRNA (c).....36

Figuer 3-3-4 *In vitro* translation inhibition assay 38

Figure 4-3-1 Amino acid sequence alignment of TTC0125 and the “reviewed” VapCs in the Uniprot database 49

Figure 4-3-2 Growth inhibition assay of TTC0125 mutants 51

Figure 4-3-3 Three-dimensional model of TTC0125 constructed by the Phyre2 program 52

Figure 4-3-4 Purification of the purified TTC0125 mutants 53

Figure 4-3-5 RNA-degrading assay of the purified TTC0125 mutants 54

Figure 5-2-1 Strategy for single TTC0125 gene disruption using *pyrE* (a) and other genes deletion using *hph5* (b) 64

Figure 5-3-1 Stress assay of *T. thermophilus* on TM agar plates containing 6 μg/ml kanamycin, 0.5 μg/ml ampicillin, 2 μg/ml chloramphenicol, 1 % NaCl, 1 μg/ml doxycycline, and 0.03% H_2O_2, respectively.....70

Figure 5-3-2 Identification of an operon including TTC0125-TTC0126 by RT-PCR 71

CHAPTER I - INTRODUCTION

Section I - Thermophiles and Evolution of Life

1-1-1 Ancestral life

Theoretical studies for the origin of life and its early evolution are the key to understanding about life. The first chemical traces of life had been found in the rocks from Precambrian deep-sea vents, at times between 3.5 and 3.9 Gyr ago (Stetter, 2006). Microfossils whose structures showed remarkable resemblance to bacteria and cyanobacteria, found in Apex cherts of the Warrawoona Group in Western Australia from ~3,465-million-year-old, currently provide the oldest morphological evidence for life on Earth (Brasier et al., 2002). These had been the times at the end of the heavy meteorite bombardment. The surface of the early Earth must have been much hotter than today (Stetter, 2006). Only superheat-loving microbes similar to the hyperthermophiles would have been able to thrive and survive in such an 'early times of life' scenario (Stetter, 2006).

Those of hyperthermophilic archaea and bacteria are found at the deepest and shortest branches in the phylogenetic trees, located near "origin of life", and therefore it has been proposed that the common ancestors of Archaea and Bacteria were hyperthermophilic (Akanuma et al., 2013; Pace, 1991; Stetter, 2006; Woese, 1987).

Not only theoretical studies, but the experimental support for the existence of a thermophilic universal common ancestor was supplied (Akanuma et al., 2013).

Akanuma et al present the thermal stabilities and catalytic efficiencies of nucleoside diphosphate kinases (NDK), designed using the information contained in predictive phylogenetic trees, that seem to represent the last common ancestors of Archaea and of Bacteria. These enzymes display extreme thermal stabilities, therefore it has been proposed that the common ancestors of Archaea and Bacteria were hyperthermophilic (Akanuma et al., 2013).

1-1-2 Thermophiles

Thermophiles and hyperthermophiles are present in various regions of the Earth, including volcanic environments, hot springs, mud pots, fumaroles, geysers, coastal thermal springs, and even deep-sea hydrothermal vents (Urbieta et al., 2015). The first thermophiles which exhibited unprecedented optimal growth temperatures above 80°C were isolated thirty-five years ago (Stetter, 2006). Hot springs are one of the main sites where hyperthermophiles and thermophiles are isolated, although they can also thrive in man-made environments, such as the compost facilities (Rastogi et al., 2010; Urbieta et al., 2015). From then thermophiles had turned out to be very common in geothermal environmet and deepsea. Currently, only two bacterial families are categorized as hyperthermophiles (*Aquificaceae* and *Thermotogaceae*), while the majority of hyperthermophiles are *Archaea* (Urbieta et al., 2015).

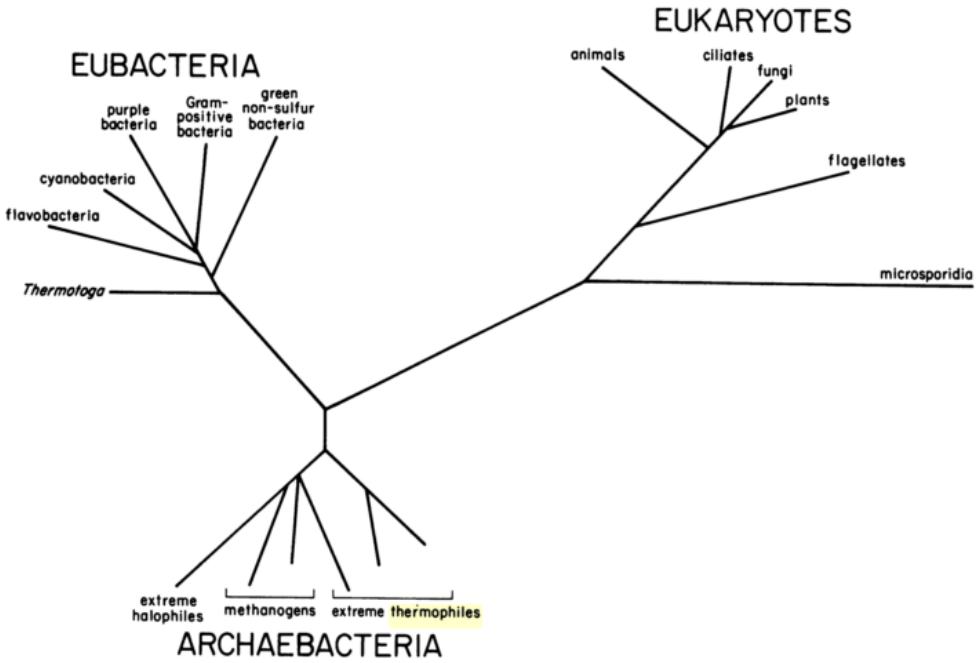

Figure 1-1-1 Universal phylogenetic tree determined from rRNA sequence comparisons (Woese et al, 1987).

Section II - *Thermus thermophilus*

1-2-1 The phylum Deinococcus-Thermus

Deinococcus-Thermus is a phylum of bacteria, which are highly resistant to environmental hazards. This phylum is a distinct branch of bacteria (Griffiths and Gupta 2007), which includes two genus of extremophilic bacteria: the thermophilic order thermales named *Thermus* and the highly radioresistant order *Deinococcus*. The genus *Deinococcus* includes at least eleven, mostly mesophilic species known for their extreme resistance to γ-irradiation and other agents causing DNA damage (Omelchenko et al. 2005), and the genus *Thermus* currently consists of 14 species.

1-2-2 Thermus thermophilus

Thermus spp. are belong to *Deinococcus-Thermus* group. They are aerobic, rod-shaped, nonsporulating, gram-negative bacteria, and most of *Thermus* species grew at an optiomum temperature of between 70°C and 75 °C, with pH ranges between 7.5 and 8.0 (Koyama, Hoshino, Tomizuka, & Furukawa, 1986). *Thermus* species use several substrates for growth, including carbohydrates, amino acids, carboxylic acids, and peptides (R. Huber *et al.* 2004), and no strain of *Thermus* appears to be capable of fermentation (R. Huber *et al.* 2004).The natural genetic competence of many *Thermus* strains makes it possible to carry out genetic studies of these organisms, and also to construct expression systems of heterologous thermophilic genes (Takayama, Kosuge, Maseda, Nakamura, & Hoshino, 2004).

The gram-negative bacterium *Thermus thermophilus*, was isolated from hot spring

in Japan (Henne et al. 2004; Oshima and Imahori 1974), which can grow up to 85 ºC. This organism has been known as an extremely thermophilic model organism, as many thermostable proteins isolated from members of the genus *Thermus* are indispensable in research and in industrial applications (Henne et al., 2004). *T. thermophilus* also has aroused interest for structural biological researchers. For example, "Structural-Biological Whole Cell Project" which I participated in Japan aims to understand all biological phenomena in the cell of one strain of *T. thermophilus*. Now several kinds of proteins have been crystallized and used for X-ray crystallographic analyses. As biomolecule structure informational advances and the coming determinate collaboration with groups of bioinformatics, *T. thermophilus* is expected to be an important model organism for atomic biology and chemical biology, which will be a new research field in the future (Wimberly et al., 2000).

Section III - Toxin-Antitoxin System

1-3-1 Toxin-antitoxin system

Toxin-antitoxin (TA) loci are widely distributed in chromosomes and plasmids of *Bacteria* (Makarova et al. 2009) and in *Archaea* as well (Grønlund and Gerdes 1999). The chromosomes of some of these bacteria contain several TA loci, especially in one of the *Mycobacterium* species, *M. tuberculosis*, which possesses the largest number of putative TA loci on its chromosome, accounting for 79 loci (Ramage et al. 2009).

TA systems consist of two small genes that encode a low molecular weight toxic protein (toxin) which reacts with intracellular target molecules related to essential cellular processes, such as DNA replication, protein translation, membrane integrity, and cell wall synthesis (Bertram and Schuster 2014; Maisonneuve et al. 2013; Page and Peti 2016), and a cognate antitoxin protein or RNA that inhibits toxin activity.

Initially, TA loci were reported to play a role in bacterial programmed cell death for maintaining plasmid stability by killing the daughter cells that failed to inherit the plasmids (Winther and Gerdes 2011). More recently, it was recognized that the toxins play roles in response to cellular stresses (Bertram and Schuster 2014), such as amino acid starvation and the presence of antibiotics (Fauvart et al. 2011; Gerdes et al. 2005; Maisonneuve and Gerdes 2014). The vast majority of TA systems in chromosomes of *Bacteria* and *Archaea* are not redundant, likely due to each system developing different responses to specific stresses (Wang and Wood 2011).

1-3-2 Types of toxin-antitoxin system

The genetic organization of the known TA loci is in general organized into operons in which the first cistron encodes the antitoxin and the second cistron encodes the toxin. But a little exceptions to this rule are existed, one known example is the *hig* locus of Rts1, in which the upstream cistron codes for the toxin (Gerdes, 2000).

As part of antitoxins showed weak similar sequences (Ruiz-Echevarría, de Torrontegui, Giménez-Gallego, & Díaz-Orejas, 1991), and also part of non-cognate toxin-antitoxins can functionally interact (Zhu, Sharp, Kobayashi, Woychik, & Inouye, 2010), It is suggested that TA loci maybe arose from a common ancestral gene (Gerdes, 2000).

Currently, TA systems are grouped into six classes according to the mechanisms used by the antitoxins to neutralize the activities of the toxins. Toxin products of all six types are proteins, while antitoxins of them are different molecules.

Well-established TA systems has three types: type I TA system consists of a protein toxin and a small regulatory antisense RNA antitoxin, which makes base-pairs to the toxin mRNA to inhibit its translation; type II TA system consists of a stable toxin protein and an unstable antitoxin protein, which forms a protein complex with the toxin protein and inhibits the toxin activity as well as represses the transcription of TA loci; antitoxin in type III system is also a small RNA, however, different with in type I, it forms pseudoknots that bind directly to the toxin protein to block its toxic activity, instead of binds to the mRNA of toxin (Page & Peti, 2016). The most recently identified

TA systems are types IV–VI: antitoxin of type IV is also a protein and directly protects the target intracellular molecule of toxin, but never interacts with toxin protein; in the only known type V system, the antitoxin is an RNase, cleaving specifically the toxin mRNA under growth conditions; type VI is composed of a protein toxin and a protein antitoxin too, in which the antitoxin is a proteolytic adaptor protein that neutralizes toxin's toxicity by promoting its degradation by other protease (Page & Peti, 2016).

CHAPTER II – IDENTIFICATION OF PUTATIVE TOXIN-ANTITOXIN SYSTEMS IN *THERMUS THERMOPHILUS* HB27

Section I - Introduction

The type II TA system is composed of a stable toxin protein and an unstable antitoxin protein. Under normal growth conditions, the antitoxin neutralizes toxin activity by forming a stable protein complex. When an environmental stressor is present, the antitoxin protein is degraded via proteolysis such that the toxin is released from the protein complex and becomes active to target intracellular molecules, such as mRNA at the ribosomal A site (Christensen and Gerdes 2003), initiator $tRNA^{fMet}$ (Winther and Gerdes 2011), Sarcin-Ricin loop of 23S rRNA (Winther et al. 2013), and glutamyl-tRNA synthetase (Germain et al. 2013), to inhibit cell growth or cause cell death. Most type II toxins function as RNases for degrading mRNA, either in a ribosome-dependent or independent manner (Unterholzner et al. 2014), such as MazF, Kid, ChpBK, MqsR, VapC, and HicA.

VapBC of type II TA system is the most widely expanded TA family and its toxin VapC contains a PIN domain, which generally functions as a nuclease enzyme that cleaves single stranded RNA (Arcus et al. 2011).

HicAB is a novel Type II TA system family identified by Makarova et al. (2006), but little is known about its function. *Escherichia coli* HicA toxin inhibits the cell growth by mRNA degradation (Jørgensen et al. 2009), and HicA from *Burkholderia pseudomallei* and *Pseudomonas aeruginosa* induces growth arrest and persistence in the

presence of ciprofloxacin or ceftazidime (Butt et al. 2014; Li et al. 2016).

Despite many investigations in mesophilic bacteria, especially in pathogens, have been reported, the mechanisms and roles of TA systems in thermophilic bacteria are still undefined. In the toxin-antitoxin database (Shao et al. 2011), 12 TA loci are predicted in the genome of *T. thermophilus* HB27, of which seven are classified into known TA families, three (TTC1395-TTC1394, TTC1549-TTC1548, and TTC1705-TTC1704) in HicAB family and four (TTC0113-TTC0114, TTC0125-TTC0126, TTC1207-TTC1208, and TTC1804-TTC1805) in VapBC family. However, no experimental analyses on these TA loci have been provided so far. Here I report the results of genetic analyses of these seven loci.

Section II - Materials and Methods

2-2-1 Bacterial strains, plasmids and media

T. thermophilus HB27 was used for genome isolation. *E. coli* strain DH5αZ1 (DH5α harboring *attB*:: P_{lacI}^{q}-*lacI*, P_{N25}-*tetR*, Sp^r; Lutz and Bujard 1997) was used for plasmid construction and expression of toxin/TA genes from pZE21MCS2 (ColE1ori, $P_{LtetO-1}$, Kn^r; Lutz and Bujard 1997). DH5αZ1 and pZE21MCS2 were purchased from Expressys. *T. thermophilus* and *E. coli* strains were cultured in TM medium (Table 2-2-1) (Koyama et al. 1986) at 70 °C and in LB medium at 37 °C, respectively.

2-2-2 Plasmid construction

To construct plasmids expressing the toxin genes or the TA modules under the control of a strictly regulated promoter, $P_{LtetO-1}$, each toxin gene or the TA locus was PCR-amplified with the primers listed in Table 2-2-2 from the *T. thermophilus* HB27 genome. Then, fragments were digested with *Kpn*I and *Sal*I, which were added just upstream of the initiation codon and downstream of the termination codon, respectively, and cloned into the respective sites of pZE21MCS, using strain DH5*α*Z1 as a host. All plasmid constructs were confirmed by nucleotide sequencing with a CEQ8000XL DNA sequencer (Beckman-Coulter).

2-2-3 Alignment and phylogenetic analysis

Phylogenetic tree based on amino acid sequences of the 7 toxins in strain *T. thermophilus* HB27 and typeical VapC and HicA was calculated. Seven toxins in *T.*

thermophilus HB27, and several amino acid sequences showing similarities to these toxins, with VapC toxin and HicA toxin amino acid sequences were selected from the Uniprot database (http://www.uniprot.org/uniprot). These sequences were aligned by the neighbor-joining method using Clustal X software and visualized by MEGA 7 software (The names of organisms and accession mumbers were indicated as FASTA organisms and accession mumbers).

2-2-4 Growth inhibition assay

The strain DH5αZ1 harboring the pZE21MCS2 plasmid containing each toxin gene or TA locus was cultured in liquid LB medium with 50 μg/mL of kanamycin at 37ºC or 43 ºC. When the $O.D._{600}$ of the culture reached approximately 0.2, 100 ng/mL doxycycline (Dox) was added to induce gene expression. Cell growth was monitored periodically by measuring $O.D._{600}$. Three independent experiments were performed.

Table 2-2-1 TM medium

＜TM medium＞

Polypepton	4 g
Yeast Extract	2 g
NaCl	1 g
Castenholz solution*	100 ml
	1 L (pH 7.5)

＜*Castenholz solution ＞

Nitrirotriacetate	1 g
$CaSO_4 \cdot 2H_2O$	0.6 g
$MgSO_4 \cdot 7H_2O$	1 g
NaCl	0.08 g
KNO_3	1.03 g
$NaNO_3$	6.89 g
Na_2HPO_4	1.11 g
$FeCl_3$ solution (2.8 g/l)	1 ml
Nitch solution**	10 ml
	1 L (pH 8.2)

＜**Nitch solution / L＞

H_2SO_4	0.5 ml
$MnSO_4 \cdot 7H_2O$	2.2 g
$ZnSO_4 \cdot 7H_2O$	0.5 g
$CuSO_4$	0.016 g
H_3BO_4	0.5 g
$Na_2MoO_4 \cdot 2H_2O$	0.025 g
$CoCl_2 \cdot 6H_2O$	0.046 g
	1 L

Table 2-2-2. Primers used in this chapter.

Primer	Sequence (5'-3')[a]
TTC0113F-Kpn	AAAGGTACC**ATG**GGAAGGCGCTACCTCCTAGAC
TTC0113R-Sal	AAAGTCGAC**TCA**CCACAGGGTCTCCACGC
TTC0114F-Kpn	AAAGGTACC**ATG**AAGGCCTTCACCGTGCAC
TTC0125F-Kpn	AAAGGTACC**ATG**GTGCTGGACGCTTCCGC
TTC0125R-Sal	AAAGTCGAC**TCA**GGAGGGCTTCCACGCCA
TTC0126F-Kpn	AAAGGTACC**ATG**GCCCTCACCATCCGCAAC
TTC1207F-Kpn	AAAGGTACC**ATG**AGGGTCGTCCTGGACACC
TTC1207R-Sal	AAAGTCGAC**TCA**GCTCACCTCCCGCAAAAAG
TTC1208F-Kpn	AAAGGTACC**ATG**CGGCGCATTGCCCTGC
TTC1395F-Kpn	AAAGGTACC**GTG**AGCCCCCGCCTCATCC
TTC1395R-Sal	AAAGTCGAC**TCA**ACGGGATCCAAGGCGCTTTTG
TTC1394F-Kpn	AAAGGTACC**AGA**TGAGGCGGCGTTACCG
TTC1549F-Kpn	AAAGGTACC**ATG**GCCAAGGGGGGGCAC
TTC1549R-Sal	AAAGTCGAC **CTA**GAGGTTATGGAACTC
TTC1548F-Kpn	AAAGGTACC**ATG**CTCAAGTACACCGCCCTCC
TTC1705F-Kpn	AAAGGTACC**ATG**GCGAGGCGGCTTAGGC
TTC1705R-Sal	AAAGTCGAC**TCA**CTCCAGCCATTCCTCCTCCTC
TTC1704F-Kpn	AAAGGTACC**ATG**GACGGGATGGGCACCCTG
TTC1805F-Kpn	AAAGGTACC**ATG**ATGCATCGCAAGCGCGTC
TTC1805R-Sal	AAAGTCGAC**CTA**GCGTCCAGCACCACCCAG
TTC1804F-Kpn	AAAGGTACC**ATG**AGCTGGGTGGTGCTGGACGC

[a] The restriction sites introduced are underlined, and the initiation and termination codons are shown in bold.

Section III - Result

2-3-1 Analysis of TA locus in T. thermophilus

In the genome of *T. thermophilus* HB27, seven TA loci were predicted as known TA families in the toxin-antitoxin database (Shao et al. 2011). Similarity searches of these putative toxins with the validated ones in the Uniprot database indicate low to moderate similarities (Table 2-3-1): TTC0113, TTC0125, TTC1207 and TTC1804, classified in the VapC family, showed 24, 44, 12 and 13% similarity to the VapC of *Mycobacterium smegmatis* (VAPC_MYCS2) (McKenzie et al. 2012), and TTC1395, TTC1549 and TTC1705 showed 37, 13 and 42% similarity to HicA of *E. coli* (HICA_ECOLI) (Jørgensen et al. 2009). Likewise, their cognate anititoxins also showed similar results: TTC0114, TTC0126, TTC1208 and TTC1805 showed 24, 37, 18 and 47% similarity to the VapB antitoxin of *M. smegmatis* (VAPB_MYCS2), and TTC1394, TTC1548 and TTC1704 showed 27, 35 and 27% similarity to the HicB antitoxin of *E. coli* (HICB_ECOLI).

2-3-2 Phylogenetic analysis

The phylogenetic tree based on the amino acid sequences of the seven toxins from *T. thermophilus* and those from the database showed that four predicted VapC toxins are clustered with known VapC toxins, and three predicted HicA toxins are clustered with known HicA toxins (Fig. 2-3-1), confirming the results by similar research (Tabel 2-3-1) and also in accordance with the predicted results by Shao et al (2011).

2-3-2 Identification of TA systems using toxin-mediated growth inhibition assays

To test whether these seven TA loci are functional, the toxin genes were cloned with or without their cognate antitoxin genes into the plasmid pZE21MCS2, and expressed under the control of $P_{LtetO-1}$ promoter in *E. coli*. This promoter is strictly regulated in the presence of TetR repressor in strain DH5αZ1, and the expression can be induced by addition of Dox (Lutz & Bujard, 1997). *E. coli* DH5αZ1 harboring the plasmids were cultured in LB medium containing kanamycin at 43ºC, and cell growth was monitored by measuring $O.D._{600}$. At $O.D._{600} \approx 0.2$, Dox was added to induce gene expression.

As shown in Fig. 2-3-2 (a), expression of one VapC (TTC0125) and two HicA (TTC1395, TTC1549) genes strictly inhibited the cell growth, whereas that of other toxin genes had almost no effect. The growth-inhibitory effects of the former three toxin genes were more obvious at 43 °C than that at 37 °C (Figure 2-3-3). Moreover, the effects of growth inhibition by expression of toxin genes were completely cancelled by co-expression with their cognate antitoxin genes (Fig. 2-3-2 b).

Table 2-3-1 Toxin-antitoxin genes in *T. thermophilus* HB27

	Toxin	Antitoxin
	VapC	VapB
VapBC	TTC0113 (26%)*	TTC0114
	TTC0125 (41%)*	TTC0126
	TTC1207 (19%)*	TTC1208
	TTC1804 (37%)*	TTC1805

*Similarity with VAPC8_MYCBO from *Mycobacterium bovis*

TA family	Toxin	Antitoxin
	HicA	HicB
HicBA	TTC1395*(26%)	TTC1394
	TTC1549*(25%)	TTC1548
	TTC1705* (23%)	TTC1704

*Similarity with HICA_ECOLI from *E. coli*

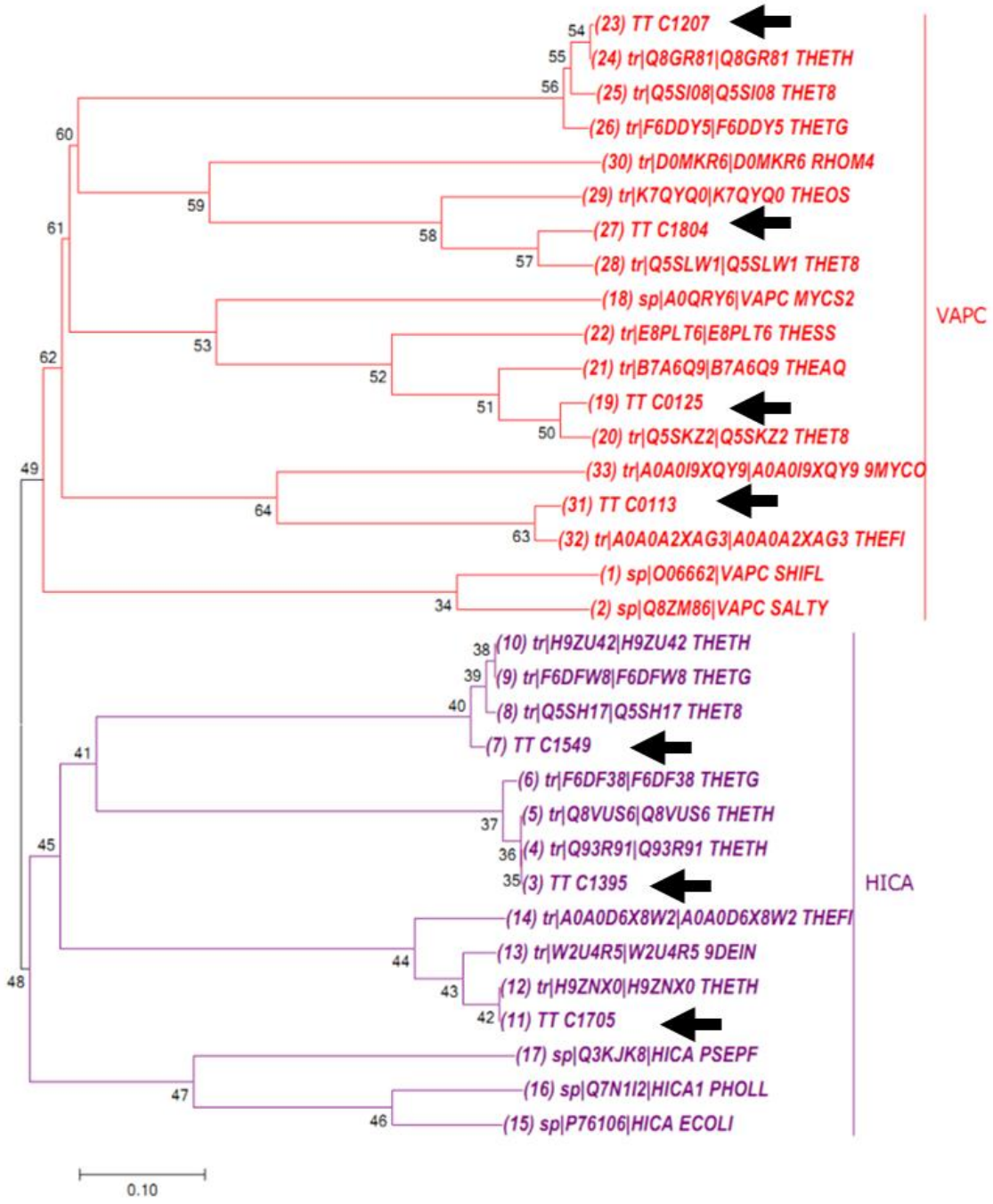

Figure 2-3-1 Phylogenetic relationships of toxin genes from *Bacteria* and *Archaea*.

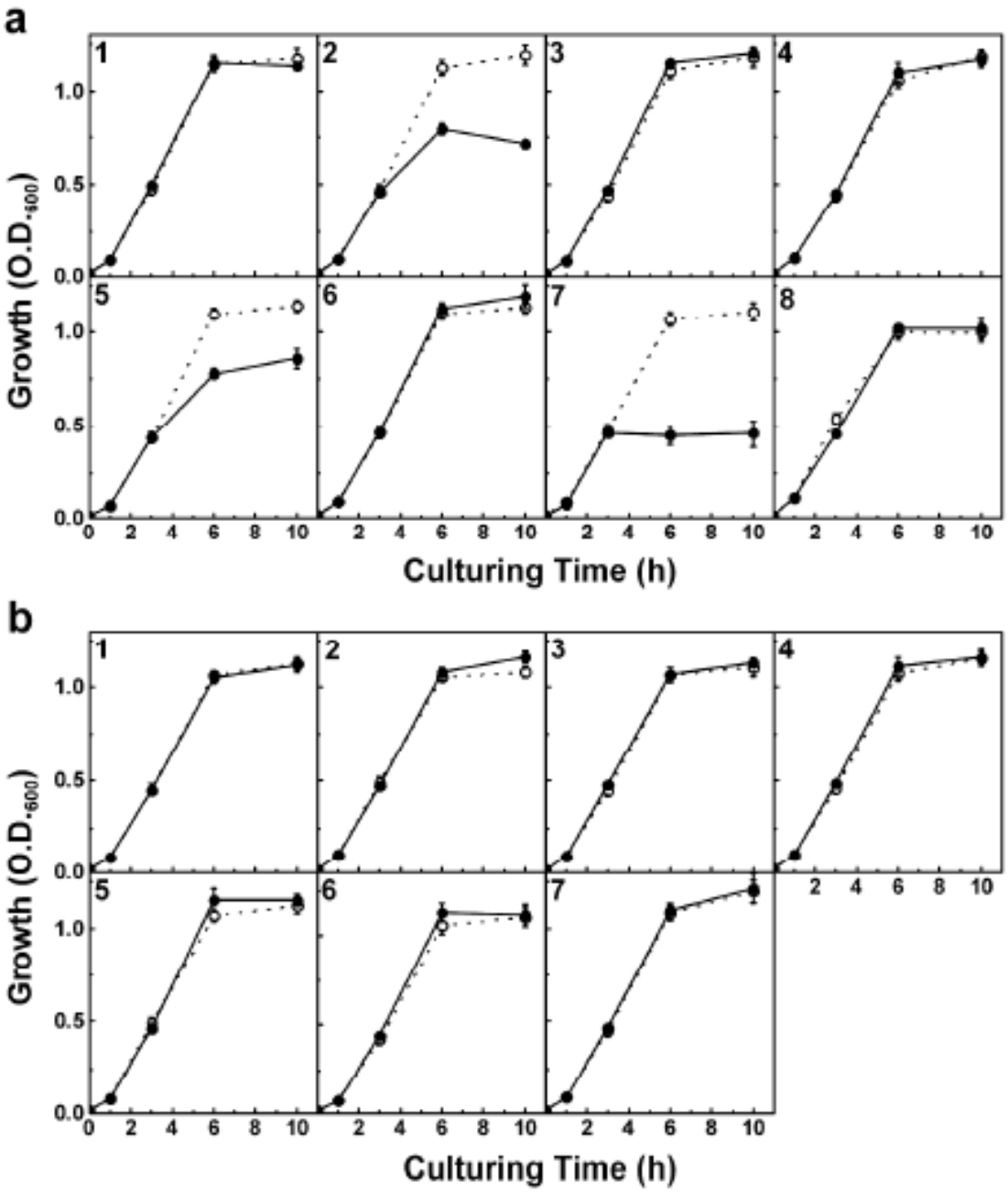
a
1
2
3
4
5
6
7
8
Growth (O.D.600)
Culturing Time (h)
b
1
2
3
4
5
6
7
Growth (O.D.600)
Culturing Time (h)

Figure 2-3-2 Growth inhibition assay.

E. coli DH5αZ1 harboring pZE21MCS2 containing toxin genes (a) of TTC0113 (1), TTC0125 (2), TTC1207 (3), TTC1804 (4), TTC1395 (5), TTC1549 (6), TTC1705 (7), or those with respective antitoxin genes (b) were cultured in LB medium containing kanamycin at 43 ºC; cell growth was monitored by measuring O.D.600. At O.D.600≈0.2, Dox was added to induce gene expression. Open circles with dotted lines indicate the culture without induction and filled circles with solid lines indicate the culture with induction. Panel (8) indicates the results from the strain harboring the vector plasmid. Culturing was conducted three times, and the mean values ±standard deviations are shown.

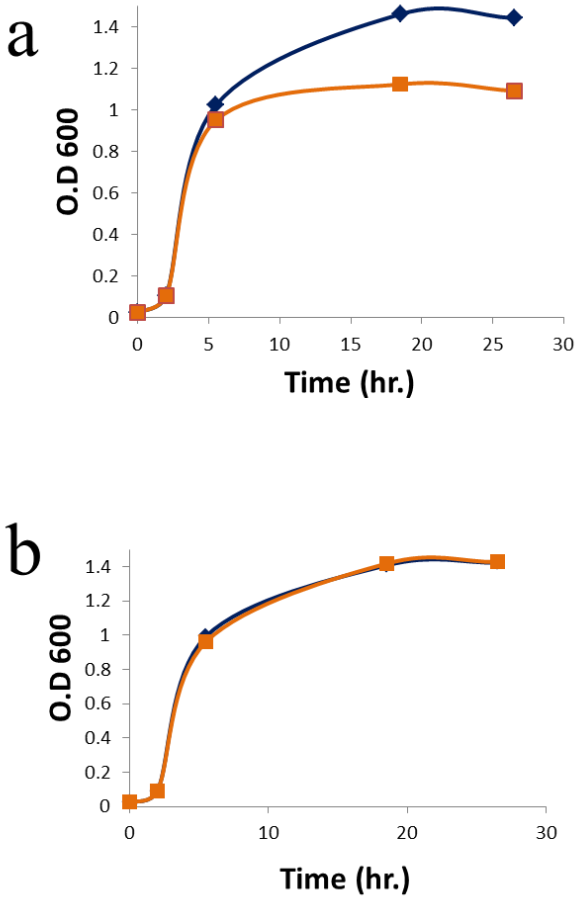

Figure 2-3-3 Growth inhibition test triggered by induction of TTC0125 (a) or TTC0125-TTC0126 (b) at 37 ºC.

E. coli DH5αZ1 harboring pZE21MCS2 containing toxin genes (a) of TTC0125 or TTC0125-TTC0126 (b) were cultured in LB medium containing kanamycin at 37 ºC; cell growth was monitored by measuring O.D.600. At O.D.600≈0.2, Dox was added to induce gene expression. Blue lines indicate the culture without induction and orange lines indicate the culture with induction.

Section IV - Discussion

In the genome of *T. thermophilus* HB27, 12 TA loci were predicted in the toxin-antitoxin database, but only seven loci were predicted as known TA families (Shao et al. 2011). To confirm these data, I did BLAST to know the similarity of the 4 predicted VapC toxin (TTC0113, TTC0125, TTC1207, and TTC1804) and 3 predicted HicA toxins (TTC1395, TTC1549 and TTC1705) with the validated toxins in the Uniprot database, and indicated that they have low-to-moderate similarities as shown in Table 2-3-1. Futhermore, I performed a phylogenetic tree based on amino acid sequences of the 7 toxins with typical VapC and HicA toxins, and showed that four predicted VapC toxins are clustered with known VapC toxins, and three predicted HicA toxins are clustered with known HicA toxins (Fig. 2-3-1), confirming that TTC0113, TTC0125, TTC1207, and TTC1804 are VapCs, and TTC1395, TTC1549, TTC1705 are HicAs.

However, there were no experimental data describing whether they are functional TA loci or not. To test whether these seven TA loci are functional, the toxin genes were cloned with or without their cognate antitoxin genes into the plasmid pZE21MCS2 and expressed under the control of the $P_{LtetO-1}$ promoter in *E. coli*. As shown in Fig. 2-3-2 (a), expression of one VapC (TTC0125) and two HicA (TTC1395, TTC1549) genes strictly inhibited cell growth, and the growth-inhibitory effects of the former three toxin genes were more evident at 43 °C than at 37 °C (Fig. 2-3-3), indicating that these toxins are more active at higher temperatures. Moreover, the effects were canceled out by co-expression of their cognate antitoxin genes (Fig. 2-3-2 b).So, I concluded that at least these three loci function as type II TA systems in *T. thermophilus*.

Additionally, as shown in Fig. 2-3-2 (a), expression of other 4 TA loci (TC0113, TTC1207, TTC1804 and TTC1549) did not affect their cell growth parttern, indicating that they are not functional, at least to 43 °C. The method used is restricted by assay temperature, as an *E. coli* strain is used as the host. Therefore, I cannot exclude the possibility that these four toxins may also possess toxin activities at higher temperatures, i.e. the growth temperature of *T. thermophilus*. One similar example is *Mycobacterium tuberculosis*, which harming 48 VapBC TA loci in its genome. Growth inhibition assay of the 48 VapBC TA loci in its genome were tested using *M. smegmatis* as a host, and showed that not all of toxins triggered significant cell growth inhibition (K. Winther, Tree, Tollervey, & Gerdes, 2016). So, I supposed that maybe the unfunctional toxins normally exist in all the genomes of microorganisms though we have not known the reason for their existence.

In this chapter, I discussed all the VapBC and HicBA TA loci in *T. thermophilus* by genetic analysis, and identified that three Type II TA loci, includes one VapBC and two HicBA, are functional TA loci, as toxin expression inhibited cell growth effectively and expression of its cognate antitoxin neutralized their effects.

In the next chapter, I will focus on the TTC0125-TTC0126 locus, the only functional VapBC TA locus in *T. thermophilus*, for further analysis.

CHAPTER III – IDENTIFICATION OF ENZYME ACTIVITY OF TTC0125-TTC0126 LOCUS

Section I – Introduction

Genetic analyses in the former chapter showed that TTC0125-TTC0126 locus is a VapBC of type II TA system, the most widely expanded TA family in *Bacteria* and *Archaea*. The VapC toxin is identified by containing a PIN domain, which generally functions as a nuclease enzyme that cleaves single stranded RNA (Arcus et al. 2011). Proteins of PIN-domain family are included in eukaryotes, eubacteria and archaea, and often be found in most of prokaryotic organisms including many famous pathogens. For example, *M. tuberculosis*, one of the most devastating pathogenic bacteria, contains 45 VapBC loci (Arcus et al. 2011), but most of them are not well characterized until now. PIN domain is identified by three highly conserved negatively-charged amino acids, and is predicted to have an RNase activity (Arcus et al. 2011). VapC toxins from different organisms were reported to have different target specificities. For example, VapC20 of *M. tuberculosis* inhibits translation by cleavage of 23S ribosomal RNA (Winther et al. 2013), and both VapC of *Shigella flexneri* and VapCLT2 of *Salmonella enterica* site-specifically cleave initiator tRNA (Winther and Gerdes 2011). On the other hand, VapC-mt4 of *M. tuberculosis* degrades mRNA (Sharp et al. 2012).

The mechanisms and roles of VapBC in thermophilic bacteria are still undefined. I will describe biochemical analyses to identify the enzyme activity of TTC0125-TTC0126 locus and their target intracellular molecules in this chapter.

Section II - Materials and methods

3-2-1 Bacterial strains, plasmids and media

T. thermophilus HB27 was used for genome isolation and purification of total RNA. *E. coli* strain DH5αZ1 was used for plasmid construction of pET28-TTC0125-TTC0126 and pET28-TTC0126. *E. coli* strain Rosetta (DE3) was used for production of TTC0125/TTC0126 proteins with plasmid pET28a. *T. thermophilus* and *E. coli* strains were cultured in TM medium (Koyama et al. 1986) with shaking at 70 °C and LB medium at 37 °C, *respe*ctively.

3-2-2 Plasmid construction

For production and purification of TTC0125 toxin and TTC0126 anititoxin, the TA locus and TTC0126 alone were PCR-amplified with primers TTC0126 F NdeI and TTC0125 R XhoI, and TTC0126 F NdeI and TTC0126 R XhoI (Table 3-2-1), respectively. The resultant fragments were cloned into the respective sites of pET28a, giving rise to pET28-TTC0125-TTC0126 and pET28-TTC0126, respectively. In both plasmids, TTC0126 was fused in-frame with the 6xHis-tag in the vector at the N-terminus, and the *Xho*I site was located just downstream of the termination codon of TTC0125 of pET28-TTC0125-TTC0126 and TTC0126 of pET28-TTC0126.

The TT_P0042 gene encoding a β-glycosidase was PCR-amplified and cloned into pET28a, giving rise to pET28-TTP0042. This plasmid was used for *in vitro* transcription and translation assays. The *tetR* gene from *E. coli* was also cloned into pET28 to construct pET28-tetR, and used for in vitro transcription and RNase assays.

All the plasmid constructs were confirmed by nucleotide sequencing with a CEQ8000XL DNA sequencer (Beckman-Coulter).

3-2-3 Purification of TTC0125 and TTC0126

TTC0125 toxin was purified essentially according to Winther and Gerdes (2011). *E. coli* Rosetta (DE3) harboring *pET28-TTC0125-TTC0126* was cultured in LB medium supplemented with 50 μg/ml kanamycin and 20 μg/ml chloramphenicol at 30 °C. When $O.D._{600}$ reached to 0.5, 0.2 mM IPTG was added, and after further culturing for 5 h, cells were collected by centrifugation at 5,000 x g for 10 min at 4 °C. Then the cells were re-suspended in ice-cold Lysis buffer (50 mM NaH_2PO_4, 100 mM NaCl, 20 mM imidazole, 0.5 mM PMSF (SIGMA), pH7.4), and disrupted by sonication. After the cell debris was removed by centrifugation at 10,000 x g for 20 min at 4 ºC, a Ni-NTA agarose resin (Qiagen) was added to the supernatant and incubated for 2 h at 4 ºC, and subsequently loaded onto a gravity column. The column was washed extensively with Wash buffer (50 mM NaH_2PO_4, 100 mM NaCl, 20 mM imidazole, pH 7.4), and the protein complex of *TTC0125-TTC0126* was eluted with Elution buffer (50 mM NaH_2PO_4, 100 mM NaCl, 200 mM imidazole, pH 7.4). Next, the protein complex was denatured by dialyzing the complex overnight at 4 ºC with Denaturation buffer (100 mM NaH_2PO_4, 10 mM Tris–HCl, 9.8 M Urea, pH 7.4), and the solution was again loaded onto a Ni-NTA agarose column. The denatured TTC0125 was eluted in the flowthrough fraction, and refolded by subsequent four-step dialysis against: (i) 1×PBS, 0.1 % Triton X-100, 5 mM DTT, (ii) 1×PBS, 5 mM DTT, (iii) 1×PBS, 5 mM DTT, and (iv) 1× PBS, 20 % glycerol, 1 mM DTT for 4 h in each dialysis.

For purification of TTC0126, *E. coli* Rosetta (DE3) harboring pET28-TTC0126 was cultured and the cell-free extract was prepared in the same way as above. TTC0126 was purified from the extract directly with a Ni-NTA agarose. The purification steps were monitored by SDS-PAGE according to Laemmli (1970).

3-2-4 RNA degradation assay

One-hundred pmol of the purified TTC0125 protein, dialyzed against Reaction buffer (50 mM Tris-HCl, 100 mM NaCl, 10 mM $MgCl_2$, 1 mM DTT, pH 7.4) prior to the reaction, was incubated with one μg of total RNA from *E. coli* and *T. thermophilus*, prepared using a RNeasy Mini Kit (Qiagen), or an *in vitro*-transcribed *tetR* mRNA, which was prepared using pET28-tetR and an *in vitro* Transcription T7 Kit (TAKARA) and purified with RNeasy Mini Kit (Qiagen), at 50 ºC in Reaction buffer. After 5, 15, 30, or 60 min. incubation, the reaction was stopped by adding 1x loading buffer (47.5 % formamide, 0.01 % SDS, 0.01 % bromophenol blue, 0.5 mg/ml EtBr, 0.5 mM EDTA) and placed on ice immediately. Then the samples were loaded onto a denaturing agarose gel (1% agarose, 6.5% formaldehyde, 0.4 M MOPS, 100 mM sodium acetate, 10 mM EDTA) and analyzed. To test the inhibitory effect of TTC0126, 100 pmol of TTC0125 was incubated with 500 pmol of the purified TTC0126, which was also dialyzed against Reaction buffer, at 50 ºC for 15 min. prior to the reaction, and used for the assay.

For activity measurement against intact ribosomes, ribosomes were purified from *E. coli* and *T. thermophilus* cells according to Pongs (1973) and Trauner (2011). Then 10 μg of TTC0125 was incubated with 50 μg of ribosomes in Reaction buffer at

50 ºC for 60 min., and rRNA was purified with an RNeasy Mini Kit for gel electrophoresis.

For activity measurement against tRNA, the small RNA fraction containing tRNA was prepared from *E. coli*, using ISOGEN II (NIPPON GENE). Then one μg of the sample was incubated with TTC0125 as described above, and resolved by an 8% denaturing PAGE. After the sample was electroblotted onto a Hybond-N membrane, the initiator tRNA was hybridized with a biotin-labelled DNA probe, tRNAMet (Table 3-2-1). Detection was conducted with a Chemiluminescent Nucleic Acid Detection Module (Thermo) and a LAS-2000 detector (Fuji film).

3-2-5 In vitro translation inhibiton assay

An *in vitro* translation inhibition assay was performed under the following conditions, using the *in vitro* transcribed TT_P0042 mRNA, which was synthesized with pET28-TTP0042 as a template and the *in vitro* Transcription T7 Kit, and a PUREfrex 2.0 kit (GeneFrontier; Shimizu et al. 2001). For each condition, the amount of the purified TTC0125, TTC0126 proteins, and the template mRNA used were 45, 270 pmol, and 2.5 μg, and the substrate-tRNA mixture (Solution I, PUREfrex), the enzyme mixture (Solution II), and the ribosome (Solution III) solutions used were 10, 1, and 2 μl in a total volume of 20 μl, respectively.

Condition 1. The template mRNA was incubated with TTC0125 at 37 ºC for 30 min. prior to the *in vitro* translation.

Condition 2. The template mRNA was incubated with TTC0125 as above, then

TTC0126 was added and the solution was further incubated for 15 min. After that, the translation reaction was started.

Condition 3. TTC0125 and TTC0126 were mixed and incubated at 37 ºC for 15 min., then the template mRNA was added and incubated further for 30 min. After that, the translation reaction was started.

Condition 4. The ribosome (Solution III) was incubated with TTC0125 at 37 ºC for 30 min., then the translation reaction was started by adding the template mRNA, Solution I and II.

Condition 5. The ribosome was incubated with TTC0125 as above, then TTC0126 was added and the solution was further incubated for 15 min. After that, the translation reaction was started.

Condition 6. TTC0125 and TTC0126 were mixed and incubated at 37 ºC for 15 min., then the ribosome was added and incubated further for 30 min. After that, the translation reaction was started.

The *in vitro* translation reaction was performed at 37 ºC for 4 h, and the translated TT_P0042 protein, containing the His-tag at its N-terminus, was detected by Western blotting, using an anti-His antibody (Qiagen) and an ECL Prime Western Blotting Detection kit (GE Healthcare). Detection was performed using a LAS-2000 detector (Fuji film).

Table 3-2-1 Primers used in this chapter.

Primer	Sequence (5'-3')[a]
for cloning into pET28a	
TTC0126F-Nde	AAACATATGGCCCTCACCATCCGCAAC
TTC0126R-Xho	AAACTCGAGTCAGTACCCCTCCTTGCCGTAC
TTC0125R-Xho	AAACTCGAGTCAGGAGGGCTTCCACGCCA
tetRF-Nde	CCGGCATATGGCACGGCTGAACAGAGA
tetRR-Xho	CCGGCTCGAGTCAGCAAAAGGGGATGATAAG
TTP0042F-Nde	GAGAGCATATGACCGAGAACGCCGAAAAATTC
TTP0042R-Xho	AATTCTCGAGTTAGGTCTGGGCCCGCGCG
for Northern blotting	
tRNAMet probe	*biotin*-CCATCATTATGAGTGATGTG

[a] The restriction sites introduced are underlined, and the initiation and termination codons are shown in bold.

Section III – Result

3-3-1 Purification of TTC0125 and TTC0126

For purification of TTC0125, I have adopted the method described by Winther and Gerdes (2011). The TTC0125-TTC0126 protein complex was first purified from the cell extract of *E. coli* Rosetta (DE3) harboring pET28-TTC0125-TTC0126 through affinity chromatography against the 6xHis-tag attached to the N-terminus of TTC0126, and the proteins were denatured by treatment with 9.8 M urea. Then the sample was loaded again to the Ni-NTA agarose column and TTC0125 was purified in a flowthrough fraction. The purified TTC0125 was renatured by a stepwise dialysis. TTC0126 was directly purified by the affinity chromatography from the cell extract of strain Rosetta (DE3) harboring pET28-TTC0126. The purified TTC0125 and TTC0126 showed single bands on SDS-PAGE, the size of which were 14.7 and 10.0 kDa, respectively (Fig. 3-3-1).

3-3-2 TTC0125 degrades free rRNA and mRNA

VapC family proteins contain a PIN domain and function as RNases (Arcus et al. 2011). In order to assess the molecular function of TTC0125, I firstly analyzed its RNase activity using total RNA isolated from both *E. coli* (Fig. 3-3-2 a) and *T. thermophilus* (Fig. 3-3-2 b) as substrates. As shown in Fig. 3-3-2 (a) and (b), The major bands corresponding to 16S and 23S rRNA were gradually shifted to low molecular-weight fractions through the incubation time from 5 min to 60 min. (lane 1, 2,3,4) with TTC0125, indicating that TTC0125 degrades at least 16S and 23S rRNA

from both the organisms. And lane 5 showed that this degradation was completely inhibited when TTC0125 was incubated with TTC0126 prior to the reaction, showing that TTC0126 functions as antitoxin. Then I tried the same assay using *in vitro*-transcribed mRNA (*tetR* gene coded by *E. coli*) as its substrate. As shown in Fig. 3-3-2 (c), TTC0125 degraded mRNA in the same manner as total RNA. These results indicate that TTC0125 degrades free RNAs including both rRNA and mRNA.

3-3-3 TTC0125 not degrade tRNA or rRNA in intact ribosome

For some cases, VapC toxins showed strict substrate-specificities towards rRNA and tRNA. So I check TTC0125's enzyme activity toward intact ribosomes from *E. coli* and *T. thermophilus*, to examine whether TTC0125 has substrate specificities or not. After incubating intact ribosome with TTC0125 or TTC0125-TTC0126 complex, 16S/23S rRNA was isolated from reactions using RNA purification kit. As shown in Fig. 3-3-3 (a, b), TTC0125 did not degraded 16S/23S rRNA in intact ribosomes form both *E. coli* and *T. thermophilus*, even after incubation for 60 min. Then I assessed initiator tRNA cleavage. Small RNA fraction of *E. coli* isolated from the total RNA was used as the substrate of this assay, and the initiator rRNA was detected by Northern blotting (Fig. 3-3-3. c). As the same result as the rRNA in intact ribosme, even incubating with TTC0125 (lane 1-4) for 60 min, it showed no digestion for initiator tRNA. These results strongly indicate that TTC0125 does not possess substrate- or sequence-specificity, rather it degrades free RNA.

3-3-5 TTC0125 inhibits translation by degrading mRNA

To obtain some insights into *in vivo* molecular function of TTC0125, an *in vitro*-translation inhibition assay was conducted, using a PURERex kit. In this assay, an *in vitro*-transcribed *TT_P0042* mRNA was used as a template for translation, and the translated 6xHis-tagged protein was detected by Western blotting. The *in vitro*-transcribed *TT_P0042* mRNA or the *E. coli* ribosome fraction in the PURERex 2.0 kit were incubated with the TTC0125 or TTC0125-TTC0126 complex, as described in 3-2-5, and *in vitro* translation reactions were conducted by adding other components of the kit. The translated product was resolved by SDS-PAGE and detected by Western blotting with an anti-His antibody. A positive control without TTC0125 treatment (lane PC) produced a band of ca. 50.8 kDa, the size of which is in good agreement of the molecular weight of TT_P0042 with a 6x His tag. When incubating the mRNA with TTC0125 prior to translation, no protein production was detected (lane 1 and 2), as well as the negative control without the template mRNA (lane NC). On the other hand, pre-treatment of ribosome with TTC0125 did not affect the protein synthesis (lane 5 and 6). Also, pre-incubation of TTC0125 and TTC0126 did not affect translation in both cases (lane 3 and 7), showing that TTC0126 functions as the antitoxin of TTC0125 to inhibit its activity efficiently. Lanes 4 and 8 showed the result of a mutated TTC0125 (D99A) with mRNA (lane 4) or ribosome (lane 8), indicating that the D99A mutation led to complete loss of translation inhibition ability of TTC0125.

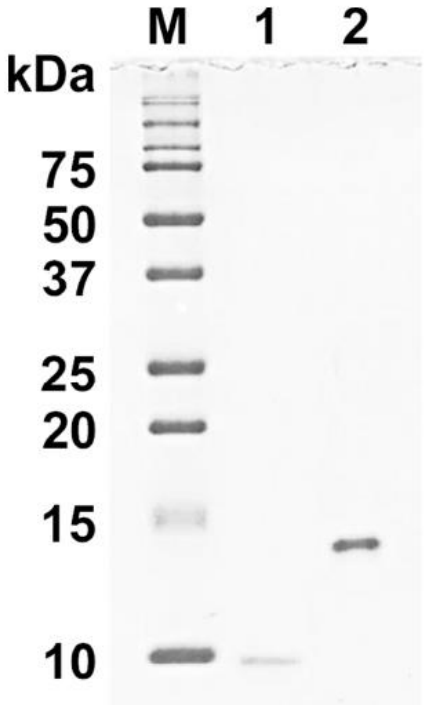

Figure 3-3-1 SDS-PAGE of the purified TTC0125 and TTC0126 proteins

Lane M, molecular marker (in kDa); 1, TTC0125; 2, TTC0126.

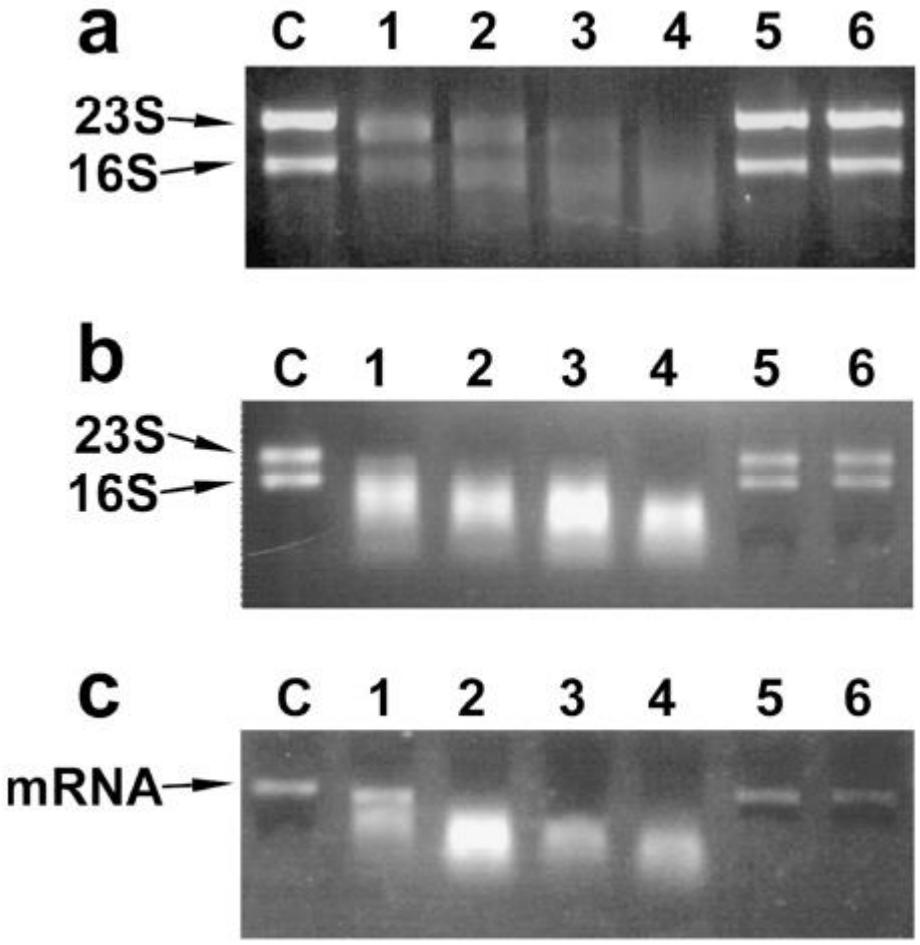

Figure 3-3-2 RNA degradation assay.

Total RNA from *E. coli* (a), *T. thermophilus* (b), and the in vitro-transcribed *tetR* mRNA (c) were incubated with the purified TTC0125 for 5 (lane 1), 10 (lane 2), 30 (lane 3), or 60 (lane 4) min, or incubated with the TTC0125-TTC0126 complex (lane 5) or TTC0125 D99A mutant (lane 6) for 60 min and electrophoresed by denaturing agarose gel. Lanes C indicate the RNA samples without TTC0125 treatment, which were also incubated in Reaction buffer for 60 min. Positions of 23S, 16S rRNA, and mRNA are indicated by arrows.

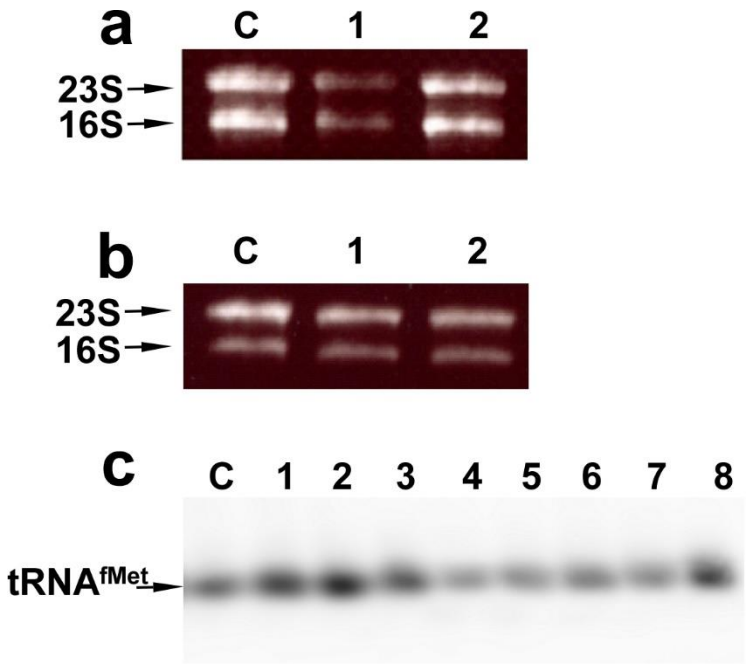

Figure 3-3-3 RNA degradation assay with intact ribosomes from *E. coli* (a), *T. thermophilus* (b), and with initiator tRNA (c).

(a, b) Intact ribosomes were incubated with TTC0125 (lane 1) or the TTC0125-TTC126 complex (lane 2) at 50 °C for 60 min. Then, RNA was prepared and loaded onto a denaturing agarose gel. Lane C indicates a control experiment in which ribosomes were incubated in the reaction buffer for 60 min. (c) Total RNA from E. coli was incubated with TTC0125 for 0 (lane 1), 15 (lane 2), 30 (lane 3), or 60 min. (lane 4), or with the TTC0125-TTC126 complex for 0 (lane 5), 15 (lane 6), 30 (lane 7), or 60 min. (lane 8), and resolved by denaturing PAGE. The initiator tRNA was detected by Northern blotting. Lane C indicates a control experiment without incubation with TTC0125. The positions of 23S, 16S rRNA, and tRNAfMet are indicated by arrows.

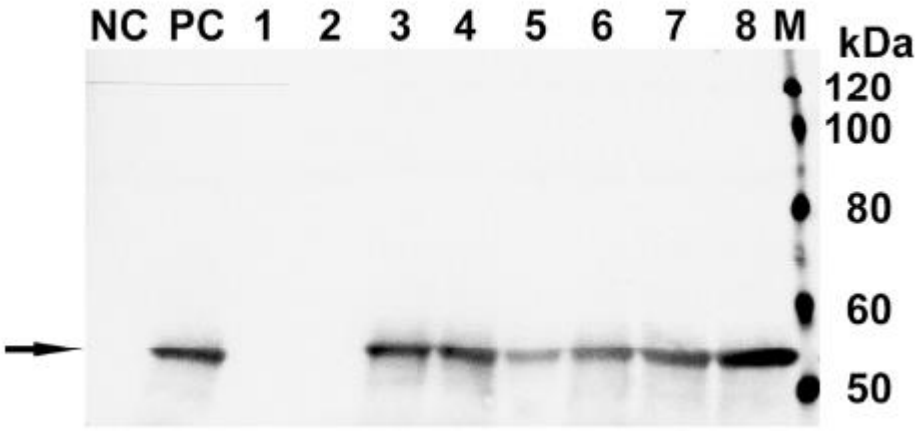
NC PC 1 2 3 4 5 6 7 8 M
kDa
120
100
80
60
50

Figuer 3-3-4 *In vitro* translation inhibition assay.

The in vitro-transcribed TT_P0042 mRNA or the E. coli ribosome fraction in the PURERex 2.0 kit were incubated with the TTC0125 or TTC0125-TTC0126 complex, as described in Materials and methods, and in vitro translation reactions were conducted by adding other components of the kit. The translated product was resolved by SDS-PAGE and detected by Western blotting with an anti-His antibody. Lane 1, the mRNA was pre-incubated with TTC0125 (Condition 1); 2, the mRNA was pre-incubated with TTC0125, and then TTC0125 –TTC0126 was added (Condition 2); 3, the mRNA was pre-incubated with TTC0125 –TTC0126 complex (Condition 3); 4, the mRNA was pre-incubated with TTC0125 D99A mutant in Condition 1; 5, the ribosome was pre-incubated with TTC0125 (Condition 4); 6, the ribosome was pre-incubated with TTC0125, and then TTC0126 was added (Condition 5); 7, the ribosome was pre-incubated with TTC0125-TTC0126 complex (Condition 6); and 8, the ribosome was pre-incubated with TTC0125 D99A mutant in Condition 4. Lanes NC and PC indicate negative control without the template mRNA addition and positive control without TTC0125 treatment, respectively. Lane M indicates the molecular marker standards (MagicMark XP Western Protein Standard, Thermo Fisher Scientific), the size of which are indicated on the right. The bands corresponding to the full-length translated product is indicated by an arrow.

Section IV - Discussion

In this chapter, I described biochemical analyses to identify the enzyme activity of TTC0125 and its target intracellular molecules.

Firstly, purification of TTC0125 and TTC0126 was conducted for biochemical analyses. Using the method described by Winther and Gerdes (2011), toxic TTC0125 protein could be produced in *E. coli* as a TTC0125-TTC0126 protein complex and purified to homogeniety.

Secondly, I identified the enzyme activity of TTC0125 using the purificated proteins of TTC0125 and TTC0126. As VapC toxin is known to possess a ribonuclease activity in mesophilic bacteria (Arcus et al. 2011), I performed an RNase assay using total RNA isolated from both *E. coli* and *T. thermophilus* as substrates (Fig. 3-3-2), and demonstrated that TTC0125 degrades at least 16S and 23S rRNA from both the organisms. TTC0126, the antitoxin of TTC0125, completely inhibited ribonuclease activity of TTC0125 by incubating them prior to the reaction. Some VapC toxins show strict substrate specificities toward rRNA and tRNA. For example, VapC20 of *M. tuberculosis* cleaves the Sarcin-Ricin loop of 23S rRNA in intact ribosome (Winther et al. 2013), and VapC (MvpT) of *Shigella flexneri* cleaves the anticodon loop of the initiator tRNA (Winther and Gerdes 2011). To examine whether TTC0125 has such substrate specificities or not, I first checked its activity toward intact ribosomes from *E. coli* and *T. thermophilus* (Fig. 3-3-3 a, b). The result showed that TTC0125 did not cleave or degrade ribosomes. For assessment of initiator tRNA cleavage, the initiator tRNA of *E. coli* was detected by Northern blot hybridization, and showed that TTC0125

did not react with the initiator tRNA (Fig. 3-3-3 c). On the other hand, TTC0125 degrades *in vitro*-transcribed mRNA of *E. coli* gene (*tetR*) in the same manner as total RNA (Fig. 3-3-2 c). These results strongly indicate that TTC0125 does not have any substrate and sequence specificity, rather it degrades free RNA, such as VapC6 of *Sulfolobus solfataricus* (Maezato et al. 2011) and those of some pathogenic bacteria (Daines et al. 2007; Ramage et al. 2009).

Moreover, to obtain some insights into *in vivo* molecular function of TTC0125, an *in vitro*-translation inhibition assay was conducted, using a PURERex kit. As prediceted, there was no band observed for negative control (fig. 3-3-4 lane NC) without addition of tempalate mRNA. On the contrast, a positive control experiment with template *tetR* mRNA addition of but without TTC0125 addition produced a band of ca. 50.8 kDa corresponding to the molecular weight of TT_P0042 protein with a 6×His-tag (Fig. 3-3-4 lane PC). When the mRNA was incubated with TTC0125 prior to translation, the band was not observed (Fig. 3-3-4 lane 1). Also, the band was not observed when TTC0126 was added after incubation of the mRNA with TTC0125 (Fig. 3-3-4 lane 2). However, TT_P0042 protein was successfully translated when the mRNA was incubated with the TTC0125-TTC0126 complex (Fig. 3-3-4 lane 3). It seems likely that TTC0125 inhibits translation by degrading mRNA.

On the other hand, pre-treatment of ribosome with TTC0125 resulted in decrease of the translated product (Fig. 3-3-4 lane 5), however, this decrease did not occur when TTC0126 was added to the ribosome-TTC0125 mixture before translation reaction (Fig. 3-3-4 lane 6). This observation can be explained that the active TTC0125 degrades mRNA during translation reaction, but not affect the ribosome function. Again,

pre-incubation of ribosome with TTC0125-TTC0126 did not affect translation efficiency.

In this chapter, I conclude that TTC0125 is a ribonuclease targeting free RNAs. It has no site-specific acitivity, and it inhibits translation by degrading mRNA.

CHAPTER IV – IDENTIFICATION OF CATALYTICALLY-IMPORTANT RESIDUES OF TTC0125

Section I - Introduction

VapC toxin contains a PIN domain of 130 amino acids in length and is predicted to have a ribonuclease activity. The Pfam database (Finn et al., 2010) identified 3457 proteins belonging to the PIN-domain family (PF01850) from 490 different species including eukaryotes, eubacteria and archaea. Several structural analyses of PIN proteins indicated the active sites containing three strictly conversed amino acids consisting of two Asp and one Glu. And Prat VapCs contains other two less conversed amino acids of Asp placed in their C terminal region (Arcus et al. 2004b; Arcus et al. 2011; Bunker et al. 2008; Das et al. 2014; Dienemann et al. 2011; Lee et al. 2015; Min et al. 2012). In recent years several structural analyses and experimental results demonstrated that the three conversed amino acid residues are important for their activity of PIN domain proteins (Hamilton, Manzella, Schmidt, DiMarco, & Butler, 2014; Sharp et al., 2012b; K. S. Winther & Gerdes, 2011a), but other amino acid residues that may have important roles for the activity are not be paid attention sufficiently. Moreover, these studies only showed their role for toxin activity by expressing mutants of these amino acids *in vivo*, however, their role for enzyme activity has not been demonstrated until now. So I constructed several mutants in which the conserved amino acid residues in TTC0125 and other VapCs were replaced, and analyzed their effects on enzyme activity in this chapter.

Section II - Materials and methods

4-2-1 Bacterial strains, plasmids and media

T. thermophilus HB27 was used for genome isolation and purification of total RNA. *E. coli* strains DH5αZ1 (DH5α harboring *attB*:: P_{lacI}^{q}-*lacI*, P_{N25}-*tetR*, Sp^r; Lutz and Bujard 1997) and Rosetta (DE3) were used for plasmid construction and expression of mutated TTC0125 from pZE21MCS2 (ColE1*ori*, $P_{LtetO-1}$, Kn^r; Lutz and Bujard 1997), and production of mutant proteins with pET28a, respectively. *T. thermophilus* and *E. coli* strains were cultured in TM medium (Koyama et al. 1986) with shaking at 70 °C and LB medium at 37 °C, respectively.

4-2-2 Site-directed mutagenesis

Single amino acid-substitution mutants of TTC0125 were constructed using pZE21MCS2 plasmid harboring TTC0125 and pET28-TTC0125-TTC0126 as templates, primers listed in Table 4-2-1, and a QuickChange site-directed mutagenesis kit (Agilent Technologies). The resultant pZE21MCS2 plasmids harboring the mutant TTC0125 were used for the growth inhibition assay, and pET28-TTC0125-TTC0126 harboring mutant genes were for protein purification and biochemical assays.

4-2-3 Growth inhibition assay

Strain DH5αZ1 harboring pZE21MCS2 plasmid containing the mutant genes was cultured in liquid LB medium with 50 μg/ml of kanamycin at 43 ºC. When $O.D._{600}$ of the culture reached around 0.2, 100 ng/ml doxycycline (Dox) was added to induce

gene expression. Cell growth was monitored periodically by measuring $O.D._{600}$. Three independent experiments were performed.

4-2-4 RNA degradation assay

One-hundred pmol of the wild type or mutated TTC0125 protein, dialyzed against Reaction buffer (50 mM Tris-HCl, 100 mM NaCl, 10 mM $MgCl_2$, 1 mM DTT, pH 7.4) prior to the reaction, was incubated with one μg of total RNA from *E. coli* and *T. thermophilus*, prepared using a RNeasy Mini Kit (Qiagen) at 50 ºC in Reaction buffer. After 60 min. incubation, the reaction was stopped by adding 1x loading buffer (47.5 % formamide, 0.01 % SDS, 0.01 % bromophenol blue, 0.5 mg/ml EtBr, 0.5 mM EDTA) and placed on ice immediately. Then the samples were loaded onto a denaturing agarose gel (1% agarose, 6.5% formaldehyde, 0.4 M MOPS, 100 mM sodium acetate, 10 mM EDTA) and analyzed.

Table 4-2-1 Primers used in this chapter.

Primer	Sequence (5'-3')[a]
D4AF	GCCATATGGTGCTGG*C*CGCTTCCGC
D4AR	GCGGAAGCG*G*CCAGCACCATATGGC
E23AF	GAGGAGCTTTTGG*C*GGAACTCCGGCG
E23AR	CGCCGGAGTTCC*G*CCAAAAGCTCCTC
E40AF	CCACCCTGGCCG*C*AGCGGGGATCGTC
E40AR	GACGATCCCCGCT*G*CGGCCAGGGTGG
F71AF	CCGAGATCGTGCCC*GC*TACCGAAAGGCATG
F71AR	CATGCCTTTCGGTA*GC*GGGCACGATCTCGG
T72AF	GATCGTGCCCTTT*G*CCGAAAGGCATG
T72AR	CATGCCTTTCGG*C*AAAGGGCACGATC
A76DF	CCGAAAGGCATG*A*CCGGGAGGCCATC
A76DR	GATGGCCTCCCGG*T*CATGCCTTTCGG
G94DF	GGCACCCCGCCG*AT*CTCAACTTCGGG
G94DR	CCCGAAGTTGAG*AT*CGGCGGGGTGCC
G98DF	GGGCTCAACTTCGACG*AC*TGCCTGAGC
G98DR	GCTCAGGCAGTC*GT*CGAAGTTGAGCCC
D99AF	CTCAACTTCGGGG*C*CTGCCTGAGCTAC
D99AR	GTAGCTCAGGCAG*G*CCCCGAAGTTGAG
S102DF	GGGACTGCCTG*GAT*TACGCCCTGGCC
S102DR	GGCCAGGGCGTA*ATC*CAGGCAGTCCC
L105DF	CTGAGCTACGCC*GAC*GCCCGGGTGGAG
L105DR	CTCCACCCGGGC*GTC*GGCGTAGCTCAG
V108DF	CCCTGGCCCGGG*AC*GAGGGGGAACC
V108DR	GGTTCCCCCTC*GT*CCCGGGCCAGGG
D119AF	CTACAAGGGCCAGG*C*CTTTGACCGGACG
D119AR	CGTCCGGTCAAAG*G*CCTGGCCCTTGTAG
D124AF	CTTTGACCGGACGG*C*CCTGGCGTGGAAG
D124AR	CTTCCACGCCAGG*G*CCGTCCGGTCAAAG

[a] The mutations are underlined and shown in italics.

Section III – Result

4-3-1 Conserved amino acid residues of VapCs

An amino acid sequence alignment of TTC0125 with some “reviewed” VapCs in the Uniprot database was generated by the T-Coffee program (Notredame et al. 2000). Conserved residues are shaded, of which those conserved among all the sequences are in black. As shown in Fig. 4-3-1, the putative active sites in all PIN domain proteins, D4, E40 and D99, are also conserved in TTC0125, indicated that TTC0125 have a PIN domain. And some amino residues like D119 and D124 are reported to be active sites in some VapCs, though they are not tightly conserved.

To find the important amino residues for enzyme activity, I chose the Asp (D119 and D124) exist near the C terminator in the alignment, and part of slightly conserved amino residues as well as tightly conserved catalytic ones. I conducted site-directed mutagenesis to introduce single amino acid substitutions of these residues to Ala or Asp, constructed mutants named D4A, E23A, E40A, F71A, T72A, A76D, G94D, G98D, D99A, S102D, L105D, V108D, D119A and D124A. All the Amino acid substitutions introduced in TTC0125 in this study are indicated above the alignment by arrows (Fig. 4-3-1). The mutant genes were introduced into *E. coli* DH5αZ1 on pZE21MCS2.

4-3-2 *Growth inhibition assay of TTC0125 mutants.*

E. coli DH5αZ1 harboring the resultant pZE21MCS2 plasmids containing the mutant TTC0125 were used for the growth inhibition assay. As shown in Fig. 4-3-2, the

E23A, T72A, L105D, and V108D mutants showed similar growth inhibition as the wild type TTC0125 gene, suggesting that these residues are not required for its toxin activity. The F71A mutant showed a weaker growth inhibition, suggesting that this residue may be required for this activity to some extent. In contrast, the D4A, E40A, A76D, G94D, G98D, D99A, S102D, D119A, and D124A mutants, including the mutants of the putative catalytic residues, had almost no effect on cell growth, demonstrating the importance of these residues for its in vivo toxin activity.

4-3-3 *Three-dimensional model of TTC0125*

As the three-dimensional structure of TTC0125 is currently not available, I have developed a three-dimensional model, using the Phyre2 program (Kelly et al. 2015), to obtain some insight into structure-activity relationship of TTC0125. The Phyre2 program indicated that TTC0125 showed 37% identity with VapC30 of *M. tuberculosis* H37Rv (PDB No. 4xgr), and a model structure of the second to 128th amino acid of TTC0125 was constructed (Fig. 4-3-3) based on that of VapC30 with a 100% confidence, indicating the accuracy of the model at some extent.

Mapping of the mutated residues on the model structure (Fig. 4-3-3) indicated that the three highly conserved putative catalytic residues (D4, E40, D99) are located at one place with nearly the same topologies and distances of the side chains with those of VapC30. D119 placed in the same putative catalytic center region. F71, A76D, G94D, G98D and S102D residues, whose mutations also caused complete or partial loss of the activity, are located around the putative catalytic center. In the case of G98, it is located adjacent to one of the catalytic residue D99. On the contrary, the E23, T72, L105 and

V108, whose mutants showed similar growth inhibition as the wild type TTC0125 were located at the other side of the protein.

4-3-4 *Purification of mutants.*

To examine the mutant proteins which lost the growth inhibition activity biochemically, the proteins were purified by the same method as the wild type TTC0125. As shown in Fig. 4-3-4, all the mutant proteins could be purified as single bands. And as they are isolated from the TTC0125-TTC126 protein complex, it showed that all the mutant proteins kept their protein binding abilities.

4-3-5 *RNase assay of mutants.*

Wild type or mutated TTC0125 protein, dialyzed against Reaction buffer prior to the reaction, was incubated with total RNA from *E. coli* at 50 ºC in Reaction buffer for 60 min. The Fig. 4-3-5 showed the result of this RNA-degradation assay. Different from the wild type TTC0125 which showed an RNase activity toward both 16S and 23S rRNA of *E. coli*, the D4A, E40A, A76D, G94D, G98D, D99A, S102D, D119A and D124A mutants completely lost the activity, as well as the result of growth inhibition assays.

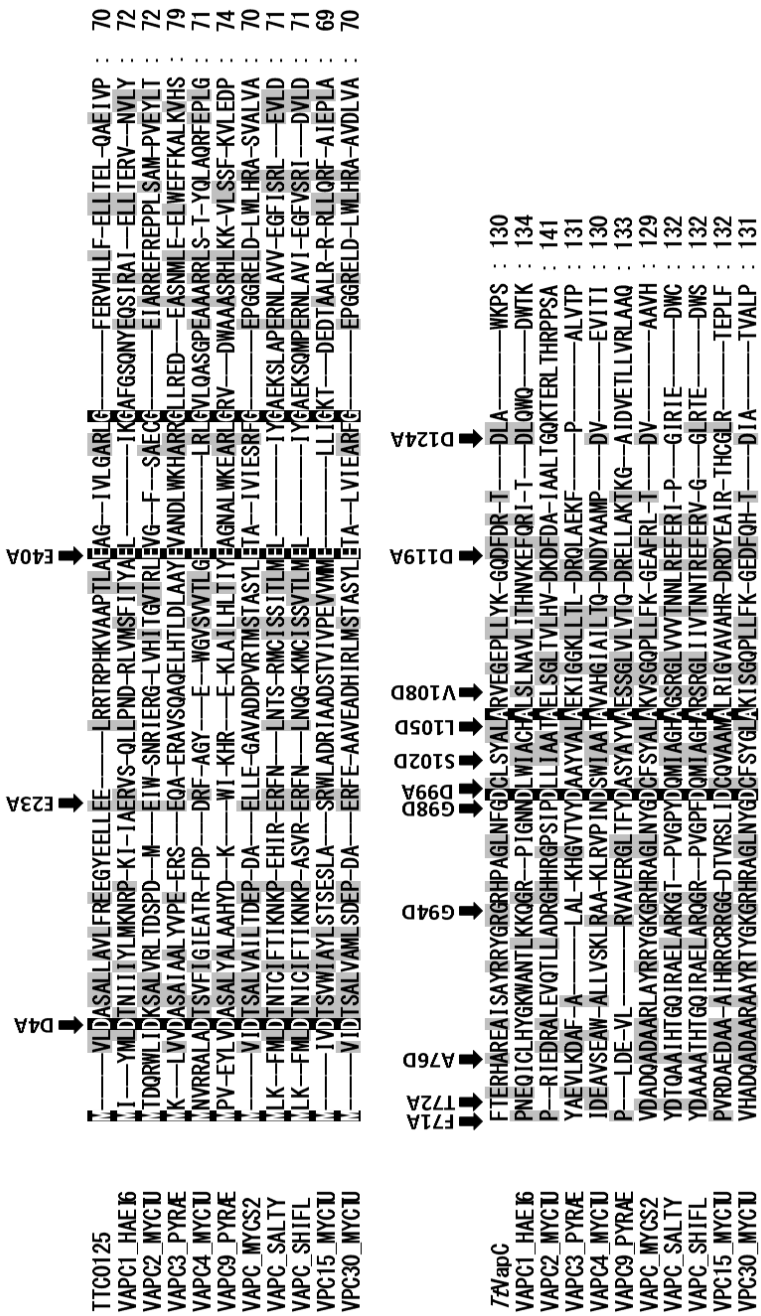

Figure 4-3-1 Amino acid sequence alignment of TTC0125 and the "reviewed" VapCs in the Uniprot database.

The alignment was generated by the T-Coffee program. Conserved residues are shaded, of which those conserved among all of the sequences are in black. Amino acid substitutions introduced in TTC0125 are indicated above the alignment.

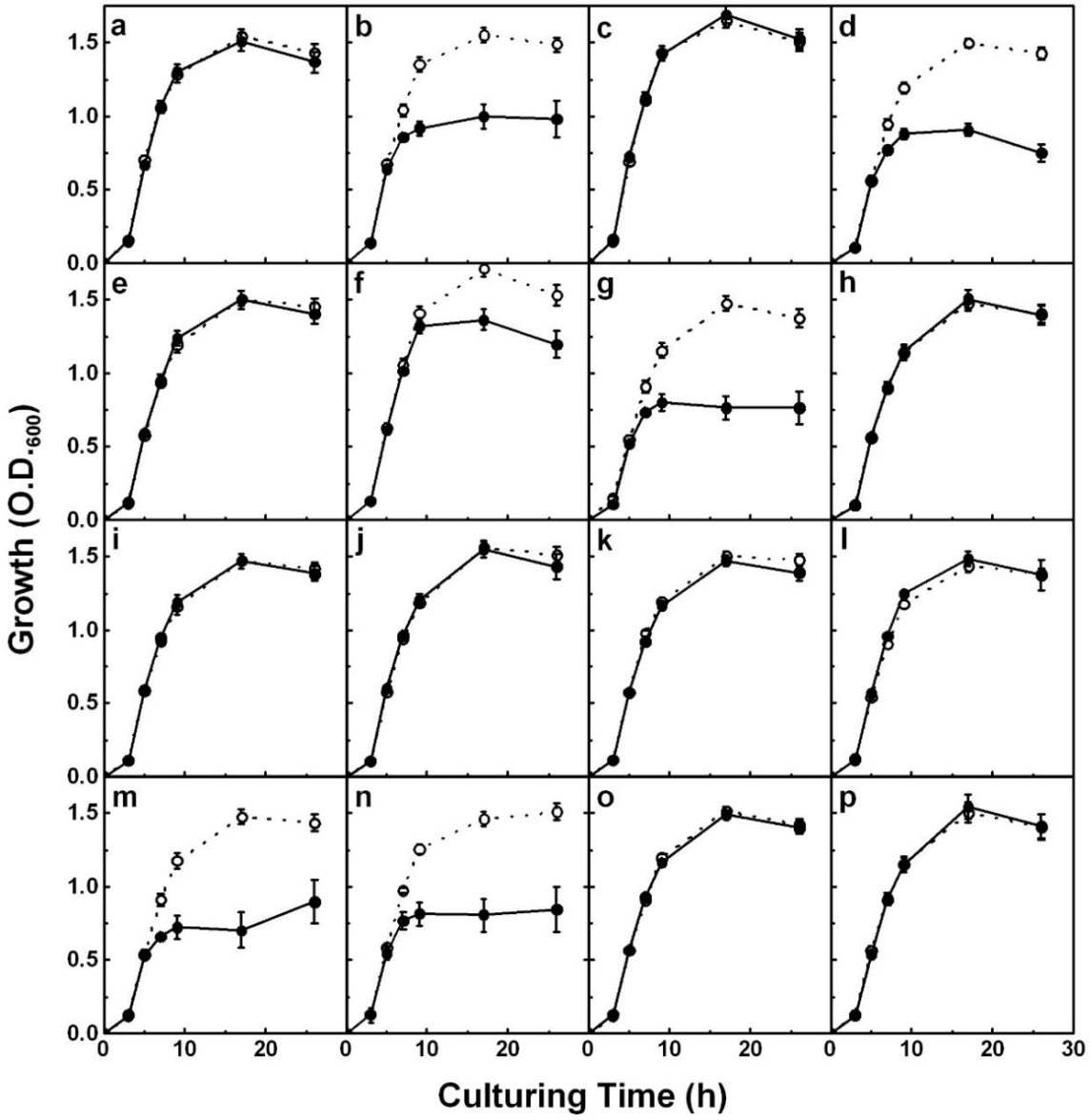
a
b
c
d
e
f
g
h
i
j
k
l
m
n
o
p
Growth (O.D.-600)
Culturing Time (h)
0.0
0.5
1.0
1.5
0
10
20
30

Figure 4-3-2 Growth inhibition assay of TTC0125 mutants.

E. coli DH5αZ1 harboring pZE21MCS2 (a), or the plasmid containing the wild type TTC0125 (b), D4A (c), E23A (d), E40A (e), F71A (f), T72A (g), A76D (h), G94D (i), G98D (j), D99A (k), S102D (l), L105D (m), V108D (n), D119A (o), or D124A (p) were cultured in LB medium containing kanamycin at 43 ºC, and cell growth was monitored by measuring O.D.600. At O.D.600 ≈ 0.2, Dox was added to induce gene expression. Open circles with dotted lines indicate the culture without induction, and filled circles with solid lines indicate the culture with induction. Culturing was conducted three times, and the mean values±standard deviations are shown.

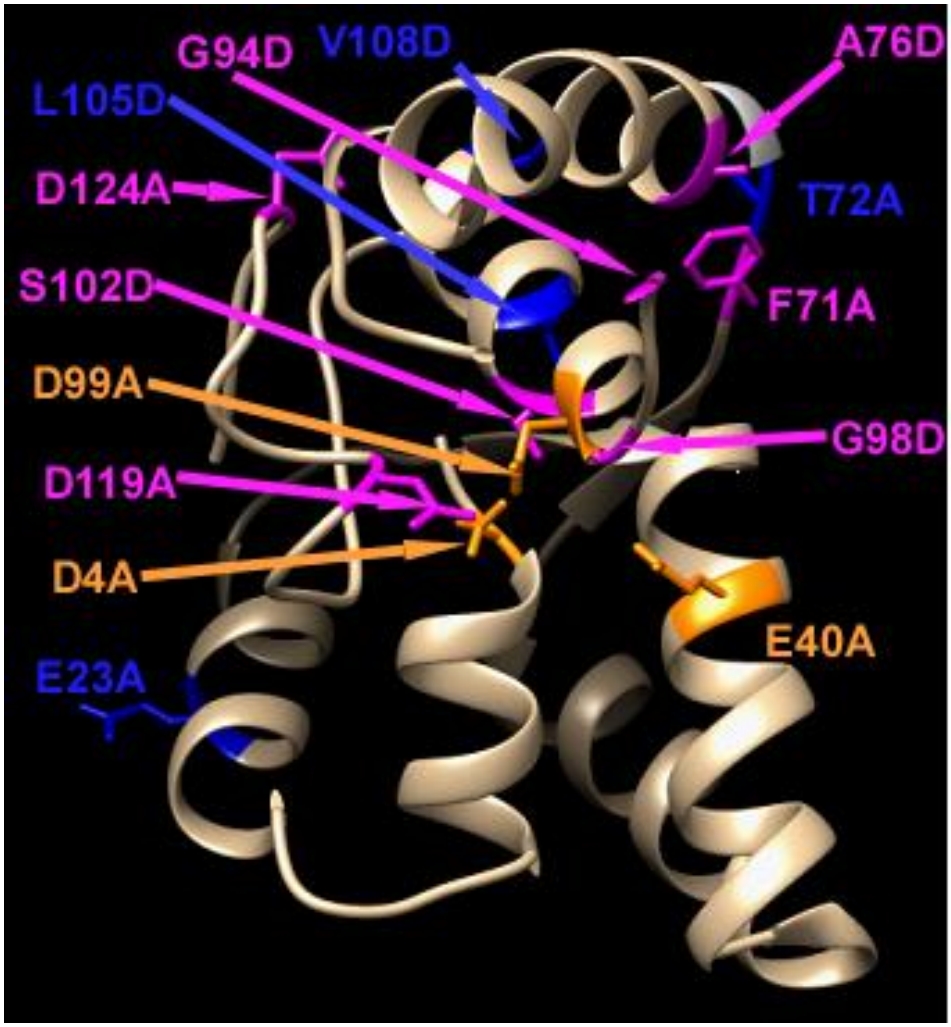

Figure 4-3-3 Three-dimensional model of TTC0125 constructed by the Phyre2 program.

Residues to which the mutations were introduced are shown with side chains and introduced mutations are indicated. Residues whose mutations affected growth inhibition activity are shown in orange and magenta, of which orange residues indicate the putative catalytic residues. Those whose mutations did not affect the activity are shown in blue.

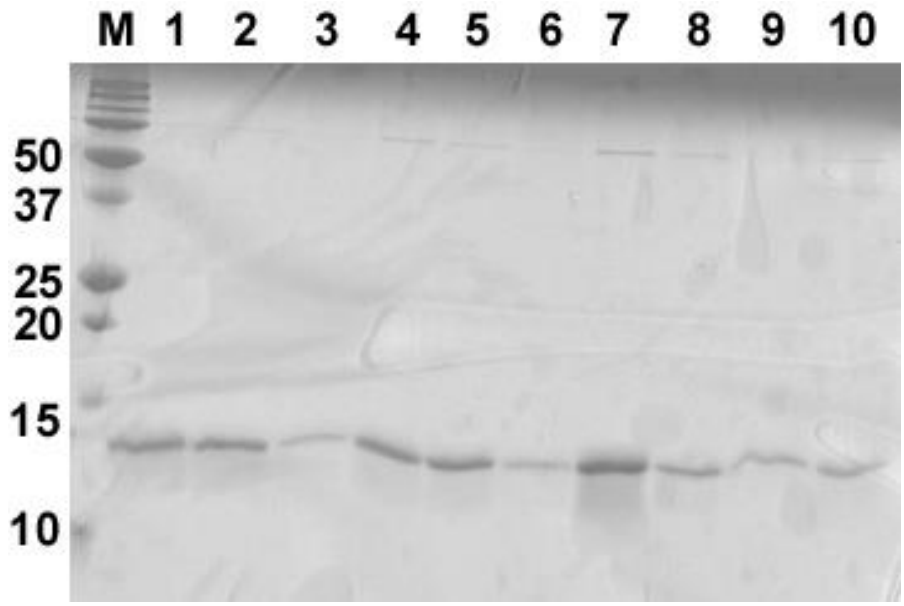

Figure 4-3-4 Purification of the purified TTC0125 mutants.

Lane 1, wild type; 2, D4A; 3, E40A; 4, A76D; 5, G94D; 6, G98D; 7, D99A; 8, S102D; 9, D119A; 10, D124A mutants. Lanes M and C indicate molecular marker (in kDa) and a control experiment without incubation with TTC0125, respectively.

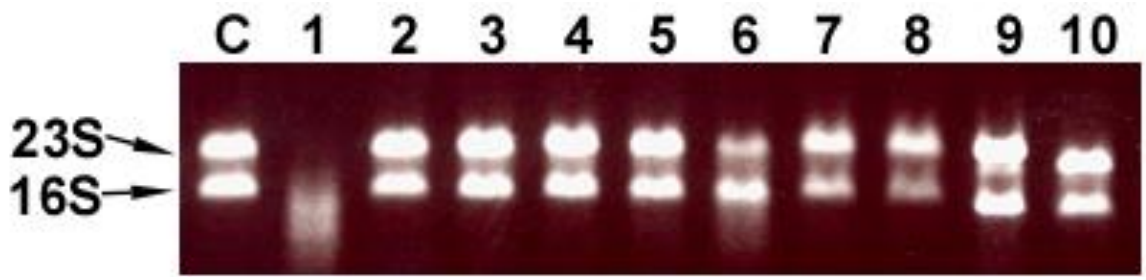

Figure 4-3-5 RNA-degrading assay of the purified TTC0125 mutants.

Lane 1, wild type TTC0125; 2, D4A; 3, E40A; 4, A76D; 5, G94D; 6, G98D; 7, D99A; 8, S102D; 9, D119A; 10, D124A mutants. Lanes M and C indicate molecular markers (in kDa) and a control experiment without TTC0125 incubation, respectively. RNA-degradation assays were conducted with E. coli total RNA, and the positions of 23S and 16S rRNA are indicated by arrows.

Section IV – Discussion

In this chapter, I conducted site-directed mutagenesis to identify catalytically-important residues of TTC0125.

An amino acid sequence alignment of TTC0125 with some “reviewed” VapCs in the Uniprot database (Fig. 4-3-1), indicates that some residues, including the putative catalytic residues in PIN proteins, D4, E40 and D99 in TTC0125 numbering, are conserved in all the VapCs. Also, some other residues are conserved in several, but not all, VapCs. I have selected such residues, including the catalytic residues, and introduced single amino acid substitutions to Ala or Asp.

Firstly, the mutant genes were used for the growth inhibition assay. As shown in Fig. 4-3-2 , the E23A, T72A, L105D, and V108D mutants showed similar growth inhibition as the wild type TTC0125 gene, suggesting that these residues are not required for its toxin activity. The F71A mutant showed a weaker growth inhibition, suggesting that this residue may be required for this activity to some extent. In contrast, the D4A, E40A, A76D, G94D, G98D, D99A, S102D, D119A, and D124A 364 mutants, including the mutants of the putative catalytic residues, had almost no effect on cell growth, demonstrating the importance of these residues for its in vivo toxin activity.

Since the three-dimensional structure of TTC0125 is currently unavailable, we developed a three-dimensional model using the Phyre2 program to gain insight into the structure-activity relationship of TTC0125 (Kelly et al. 2015). Mapping of the mutated residues on the model structure (Fig. 4-3-3) indicated that the 374 three putative

catalytic residues, whose mutations led to complete loss of growth 375 inhibition activity, are located in one place with nearly the same topologies and distances of the side chains with those of VapC30, possibly forming the catalytic center. The other residues whose mutations also resulted in complete or partial loss of activity, except for G94 and D124, are located around the putative catalytic center, suggesting 379 that these residues are involved in substrate binding or structural maintenance of the 380 putative catalytic center. In the case of G98, since the Gly residue acts as a helix breaker and this residue is located adjacent to one of the catalytic residues, D99, G98 may be required for correct positioning of D99; it remains unknown as to why the mutations of G94D and D124A lost growth inhibition activity. The E23, T72, L105, and V108 residues are located at the other side of the protein. Therefore, it is possible that mutations of these residues did not affect activity.

In order to examine the mutant proteins which lost growth inhibition activity biochemically, the proteins were purified using the same method as the wild type TTC0125. As shown in Fig. 4-3-4, all of the mutant proteins were purified as single bands. Since this purification method relies on the complex formation with TTC0126, this result indicates that the mutations introduced did not affect binding to TTC0126. As expected, all mutants lost RNase activities against total RNA (Fig. 4-3-5), and one of the mutants, D99A, as shown in chapter III, also lost activity against mRNA (Fig. 3-3-2 c) and translation- inhibition activity (Fig. 3-3-4).

Finally, I conclude that Amino acid substitutions of 14 putative catalytic and highly conserved residues in the VapC family toxins to Ala or Asp indicated that nine residues are important for its protein activity. They are D4, E40, A76, G94, G98, D99,

S102, D119 and D124. Among them, the three tightly conserved ones, D4, E40, and D99, are confirmed to be catalytic residues, as the ones reported in other VapC; A76, G94, G98, S102, D119 and D124. are confirmed to be catalytic residues experimentally by this study at first.

CHAPTER V – PHYSIOLOGICAL ANALYSES OF TTC0125-TTC0126 TA LOCUS

Section I - Introduction

TA systems are indicated to have important roles in cell physiology in *Bacteria and Archaea*. The first TA locus characterized was found in a plasmid. The cells which lost the plasmid during proliferation were killed by the toxin's action, because the 'antidote' antitoxin was highly labile compared to their cognate toxin, and the cells without the plasmid could not produce the antitoxin (Page and Peti 2016). So they prevent the proliferation of plasmid-free progeny, which increases plasmid maintenance in growing bacterial cultures (Pecota et al. 1997). However, recent researches have indicated that TA loci are ubiquitous in the free-living prokaryotic cells (Pandey and Gerdes 2005). Unlike plasmid-based TA genes, chromosomal TA loci do not mediate bacterial programmed cell death (PCD), but instead function to ensure the survival of the population in response to stress (Page and Peti 2016).

Stress induction of MazF toxin was reported to trigger the cell growth arrest, and eventually programmed cell death in *E. coli* (Aizenman et al. 1996). However, resent years' research showed that MazF not only induced gene expression required for the death of most of the cellular population, but also induced other gene expression which were found to be required for the survival of a small sub-population of cells (Amitai et al. 2009). Now, it has been established that TA systems play a central role in persistence. The first gene identified as directly affecting persistence was HicA in *E. coli*, which is a kinase that inactivates glutamyl-tRNA synthetase (Page and Peti 2016).

HipA-induced persistence depends not only on (p)ppGpp, but also on ppGpp-mediated activation of the other type II toxins, including VapBC (Germain et al. 2013, 2015).

Recent evidence indicates that TA loci function to modulate the global levels of translation and replication during exposure to some stresses, like antibiotics and amino acid starvation. For example, the activities of the TA loci YafON, HigBA and MqsRA were induced by stress conditions including serine, isoleucine or glucose starvation, and the addition of chloramphenicol or mytomycin C (Pecota et al. 1997; Yamaguchi and Inouye 2011). Under normal growth conditions, the antitoxins inhibit the activities of their cognate toxins. However, under stress conditions, the antitoxins are selectively degraded, leading to activation of toxins and therefore inhibition of essential cellular processes, such as DNA replication and protein translation.

VapBC is also observed to be induced under the stresses conditions such as amino acids starvation (Winther and Gerdes 2009), antibiotic addition (Daines, Wu, and Yuan 2007), and heat shock (Maezato et al. 2011). It is indicated that abundant VapBC TA loci exist in bacteria, especially in pathogenic ones, like *Mycobacterium tuberculosis* (Ahidjo et al. 2011) and *Rickettsia felis* (Audoly et al. 2011; Maté et al. 2012). Physiological studies demonstrate that VapBC loci in bacteria are important for adaptation to disadvantageous environments or growth conditions. Most pathogens have to make metabolic adjustments during their infection process to adapt to a change of growth condition (Cook et al. 2013). Important role of VapBC for metabolic flexibility is also confirmed in environmental microbes, as they have to adapt the changes of growth conditions. In *S. meliloti*, VapBC has been implicated in controlling bacterial growth and enhanced nitrogen fixation in root nodules by increasing transcripts of genes

involved in these cellular processes (Cook et al. 2013). And in *M. smegmatis*, which contains only one VapC, the toxin is suggested to regulate the rate of glycerol utilization to match the anabolic demands of the cell, allowing for fine-tuning of the catabolic rate at a posttranscriptional level (McKenzie et al. 2012).

No attention has been paid to physiological role of VapBC loci in thermophilic bacteria. Thus I report about it in this chapter. There are three VapBC loci in *T. thermophilus*, but only TTC0125-TTC126 locus showed functional activity, confirmed in chapter II. In this chapter, I will try to analyze the physiological role of TTC0125-TTC126 locus and report the results.

Section II - Materials and methods

5-2-1 Bacterial strains, plasmids and media

The bacterial strains used in this study are listed in Table 5-2-1. Plasmid pUC19 was used for construction of TTC0125 mutants in *T. thermophilus*. Plasmids pT8s-P31-hph5 (Nakamura et al. 2005)) and pINV (Tamakoshi et al. 1997) were sources of selection markers in *T. thermophilus*, *hph5* encoding the thermostable hygromycin B phosphotransferase and *pyrE* gene of *T. thermophilus* encoding orotate phosphoribosyl- transferase (Yamagishi et al. 1996), respectively.

T. thermophilus strains were grown at 70 ºC in a rich medium (TM) or a minimal medium (MM) (Table 5-2-2), as described earlier (Koyama et al. 1986). When necessary, proline and/or uracil (50 µg/ml each) were added to MM. *E. coli* strains were grown in Luria–Bertani (LB) medium. Kanamycin (50 µg/ml) and hygromycin (200 µg/ml) were added to the medium when necessary.

5-2-2 Disruption of TTC0125 gene and TTC0125-TTC0126 locus

To create a construct for the disruption of TTC0125 (Fig 5-2-1 a), PCR products of ~1500 bp flanking the TTC0125 gene of *T. thermophilus* was amplified using the primer TTC0125+700bp F-SalI with a restriction site *Sal*I, and TTC0125-700bp F-EcoRI with a restriction site *Eco*RI. The PCR product was digested with *Sal*I and *Eco*RI and ligated into the same sites of the pUC19 (TAKARA) plasmid to generate pUC19-1500bp. A second insert *pyrE* gene product was amplified using primers pyrE-sd-FEcoRV and pyrE-REcoRV with restriction sites *Eco*RV. This PCR product was digested with EcoRV and ligated into the *Sma*I site of the pUC19-1500bp

plasmid, to generate pUC19-del25. The plasmid pUC19-del25 thus constructed was used to transform *T. thermophilus* strain TM104 (Maehara et al. 2008), a *pyrE* mutant of TH104. After the transformants were selected on MM without uracil, correct integration was confirmed by PCR using upstream primer TTC0126 +1000bp F and downstream primer TTC0126 -1000bp R.

To create a construct for the disruption of TTC0125-TTC0126 locus (Fig 5-2-1 b), the fusion PCR technique was applied. First, two DNA fragments corresponding to ~700 bp upstream region of TTC0126 and ~700 bp downstream region of TTC0125, with 107 bp of its 3' region, were amplified using primer pairs of TTC0126+1000bpF and TTC0126+700bpR(fusionhph5), and TTC0125-100F(fusionhph5) and TTC0126-1000bpR, respectively. Also, the marker gene h*ph5* was PCR-amplified using P31-F and hph5-R, and plasmid pT8s-P31-hph5 as a template. Then, the three DNA fragments were connected by the fusion PCR using the primers TTC0126+1000bpF and TTC0126-1000bpR, to generate the disruption DNA cassette. The fusion PCR product was then used to transform *T. thermophilus* strain TM104 (Maehara et al. 2008) and the transformants selected by 40 μg/ml hygromycin in TM plates. Correct integration was confirmed by PCR using primers TTC0128F and del TTC0123R(fusion hph).

5-2-3 Reverse transcriptase PCR

Total RNA of *T. thermophius* HB27 strains was isolated using the RNeasy Mini Kit (Qiagen). Purified total RNA was treated once again by DNase I to ensure without contamination of genomic DNA, using RNase-free DNase (Qiagen). cDNA was reverse-transcribed from the total RNA using the QuantiTect Reverse Transcription Kit

(Qiagen) and the mix primers included in the kit. A 100-Fold diluted cDNA product was used as the template for the following PCR by KOD FX (Toyobo). Each sample of PCR amplification was subjected to 25 cycles and performed with the primers shown in Table 5-2-1. For excluding the effect of contamination of genome DNA, negative control was processed using the same PCR condition, with total RNA but not cDNA as a template.

5-2-4 Minimal Inhibitory Concentration (MIC) against antibiotics

MICs against several antibiotics of *T. thermophilus* were determined in duplicate according to the EUCAST broth microdilution protocol. Ampicillin, kanamycin, doxycycline and chloramphenicol (Peeters et al. 2009) concentrations ranged from 0.001 to 100 μg/ml, 0.1 to 40 and from 0.1 to 100 mg/ml, respectively, were tested. The MIC was defined as the lowest concentration for which no significant difference in optical density (600 nm) was observed between the inoculated and blank wells after 18 h incubation.

5-2-5 Biochemical Assays and Stress Experiments

Stress experiments were performed with stationary cultures grown in TM medium overnight. After standardizing to 1×10^9 /ml cells, cells were diluted to 10^8, 10^7, and 10^6 /ml cells in 0.87 % normal saline. Then 10 μl of each sample was spotted onto the TM-agar plates containing minimum inhibitory concentration (MIC) of stress reagents. All plates were incubated for up to 36 h at 65 ºC.

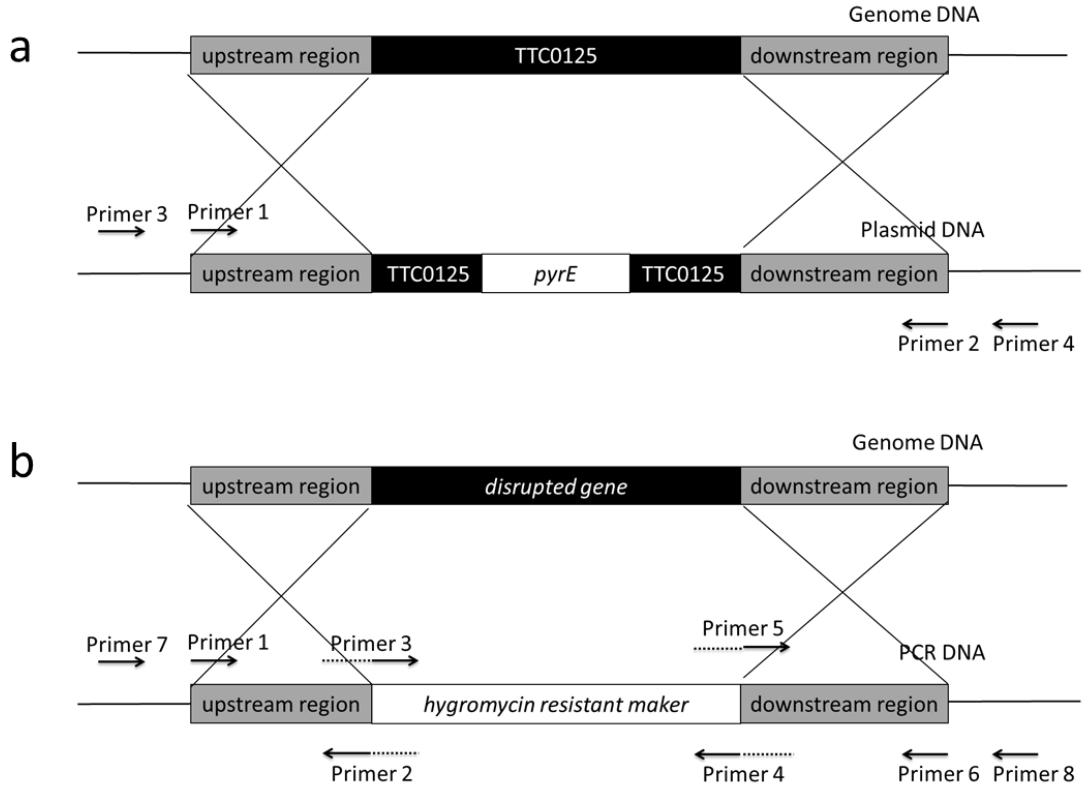

Figure 5-2-1 Strategy for single TTC0125 gene disruption using *pyrE* (a) and other genes deletion using *hph5* (b).

Table 5-2-1 Primers used in this chapter

Primer	Sequence (5'-3')
TTC0125+700bp F-SalI	ACACGTCGACTTGTGGAAGTGCCGGCACC
TTC0125-700bp F-EcoRI	ACACGAATTCGAAGGCGAGGCCGTAGCGG
pyrE-sd-F EcoRV	ACACGATATCGGCGGAGGCCCTCTTGAAGGC
pyrE-R EcoRV	ACACGATATCCTAGACCTCCTCCAAGGGCAC
TTC0126 +1000bp F	GCGAGCTCATCGCCACCTTC
TTC0126 -1000bp R	AGAGGGCGAGGAGGAACTCCAG
TC0126+1000bpF	GCGAGCTCATCGCCACCTTC
TTC0126+700bpR(fusionhph5)	GCCTTCAAGAGGGCCTCCGCCGCTTTAAGCA TGGCTGCAGGAAG
TTC0125-100F(fusionhph5)	GTGCCCTTGGAGGAGGTCTAGCTGCCTG AGCTACGCCCTGG
TTC0126-1000bpR,	AGAGGGCGAGGAGGAACTCCAG
P31-F	ATTCGGCCCAAGGTTTACAAAATCC
hph5-R	CTATTCCTTTGCCCTCGGAC
TTC0126+1000bpF	GCGAGCTCATCGCCACCTTC
TTC0126-1000bpR	AGAGGGCGAGGAGGAACTCCAG
TTC0128F	AGGTTTTGGCGGAGGACGAGGC
del TTC0123 R(fusion hph)	GATTTTGTAAACCTTGGGCCGAATTCCGT GGACGTAGAGGCTAGCCAA

Table 5-2-2 MM medium

＜TM medium＞	
Polypepton	4 g
Yeast Extract	2 g
NaCl	1 g
Castenholz solution*	100 ml
	1 L (pH 7.5)
＜*Castenholz solution ＞	
Nitrirotriacetate	1 g
$CaSO_4 \cdot 2H_2O$	0.6 g
$MgSO_4 \cdot 7H_2O$	1 g
NaCl	0.08 g
KNO_3	1.03 g
$NaNO_3$	6.89 g
Na_2HPO_4	1.11 g
$FeCl_3$ solution (2.8 g/l)	1 ml
Nitch solution**	10 ml
	1 L (pH 8.2)
＜**Nitch solution / L＞	
H_2SO_4	0.5 ml
$MnSO_4 \cdot 7H_2O$	2.2 g
$ZnSO_4 \cdot 7H_2O$	0.5 g
$CuSO_4$	0.016 g
H_3BO_4	0.5 g
$Na_2MoO_4 \cdot 2H_2O$	0.025 g
$CoCl_2 \cdot 6H_2O$	0.046 g
	1 L

Section III - Result

5-3-1 Disruption of TTC0125/TTC0125-TTC0126 changed cell response to kanamycin

To analyze the physiological function of TTC0125-TTC0126 TA locus, the gene disruption mutants of TTC0125 and TTC0125-TTC0126 locus were constructed, using *pyrE* and *hph5* genes as selection markers, respectively. The mutants were used for stress-tolerance tests as below

For antibiotic stress assay, MICs of the wild type strain against antibiotics including kanamycin, ampicillin, chloramphenicol, doxycycline were determined in advance and were used for the following stress assays. For osmotic stress assay, 1~2 % NaCl was used and for oxidation stress assay, 0.001~0.006 % of H_2O_2 was used.

As shown in Fig. 5-3-1, when the strains were cultured in the presence of 6 μg/ml kanamycin, both disruption mutants, ΔTTC0125 and ΔTTC0125-TTC126, showed increased tolerance than wild-type. And they also showed same tendency of tolerance in a range of concentration of 6~10 μg/ml kanamycin (data not show). However, to other stress condition, including other antibiotics, oxidation or osmotic, the mutants did not show any difference to the wild-type.

The result showed a phenotypic change on plate, indicating that TTC0125-TTC126 locus is involved in the stress response mechanism, *i.e.*, low dose of kanamycin, and regulates cell growth under stress.

5-3-2 TTC0125-TTC0126 locus is included in Metabolic-related operon

Analysis of the TTC0126-TTC0125 locus in *T. thermophilus* genome in KEGG database (http://www.genome.jp/kegg) revealed that the structure is like a canonical VapBC locus, in which TTC0126 antitoxin gene is preceded and TTC0125 toxin gene is followed with sharing a 1 bp overlap (Fig. 5-3-2a). However, TTC0125 is also overlapped by a downstream gene TTC0124. Moreover, a four gene cluster containing TTC0130-TTC0127 is located in the upstream region of TTC0126, with spacing of 293 bp between TTC0127 and TTC0126 ORFs. This gene organization suggests that TTC0125-TTC0126 maybe not a single, bicistronic locus as a typical VapBC locus. To test this possibility, RT-PCR assays were conducted to amplify intergenic regions of the surrounding genes of TTC0125-TTC0126 locus, using cDNA prepared from total RNA isolated from different phases of growth of *T. thermophilus* as templates.

As shown in Fig 5-3-2b, the amplified products were observed from lane 4 to lane 8, which correspond to the intergenic regions from TTC0130 to TTC0124. The negative control experiment without reverse transcription (Fig. 5-3-2 c) excluded the possibility of amplification by contamination of genome DNA. On the contrary, no bands were observed in the reaction with primers amplifying the intergenic regions of TTC0131-TTC0130 (lane 3) and TTC0124-TTC0123 (lane 9). These results confirmed that the genes from TTC0124 to TTC0130 form an operon structure in the genome of *T. thermophilus*. The annotations of the genes included in this operon are malate synthase (TTC0130), (S)-2-hydroxy-acid oxidase (TTC0127, TTC0128, TTC0129) and glycerate dehydrogenase/hydroxypyruvate reductase (TTC0124), indicating that the products of this operon are predicted to play a role to synthesize malate and related to glyoxylate

cycle. This result also revealed that there is basal level transcriptional activity of TTC0125-TTC0126 throughout the growth phase.

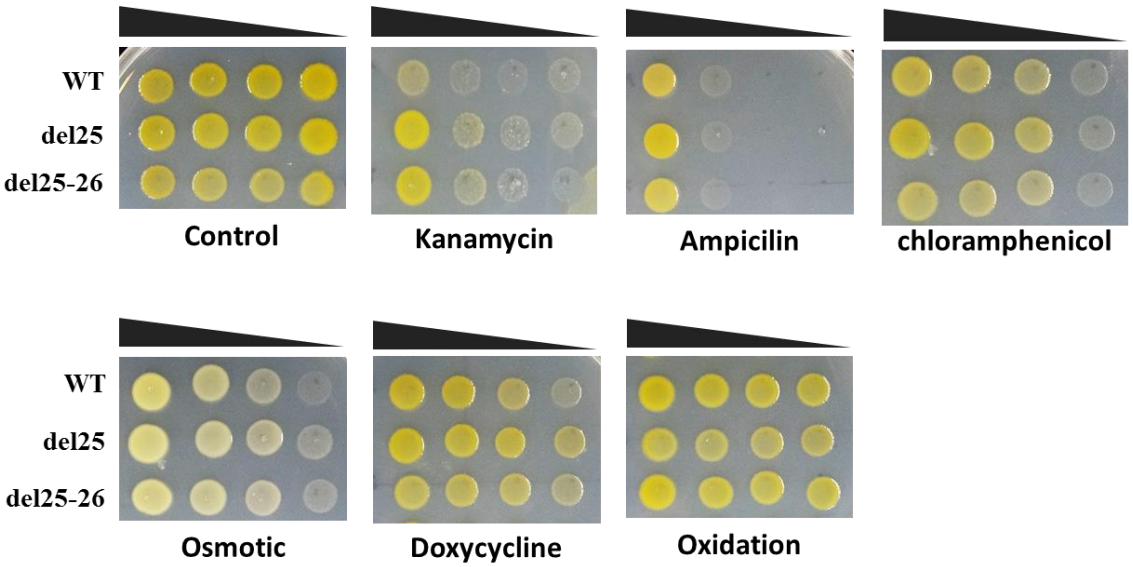

Figure 5-3-1 Stress assay of *T. thermophilus* on TM agar plates containing 6 μg/ml kanamycin, 0.5 μg/ml ampicillin, 2 μg/ml chloramphenicol, 1 % NaCl, 1 μg/ml doxycycline, and 0.03% H_2O_2, respectively. WT, wild type; del25, disruption mutant of TTC0125 gene; del25-26, deletion mutant of TTC0125-TTC0126 locus.

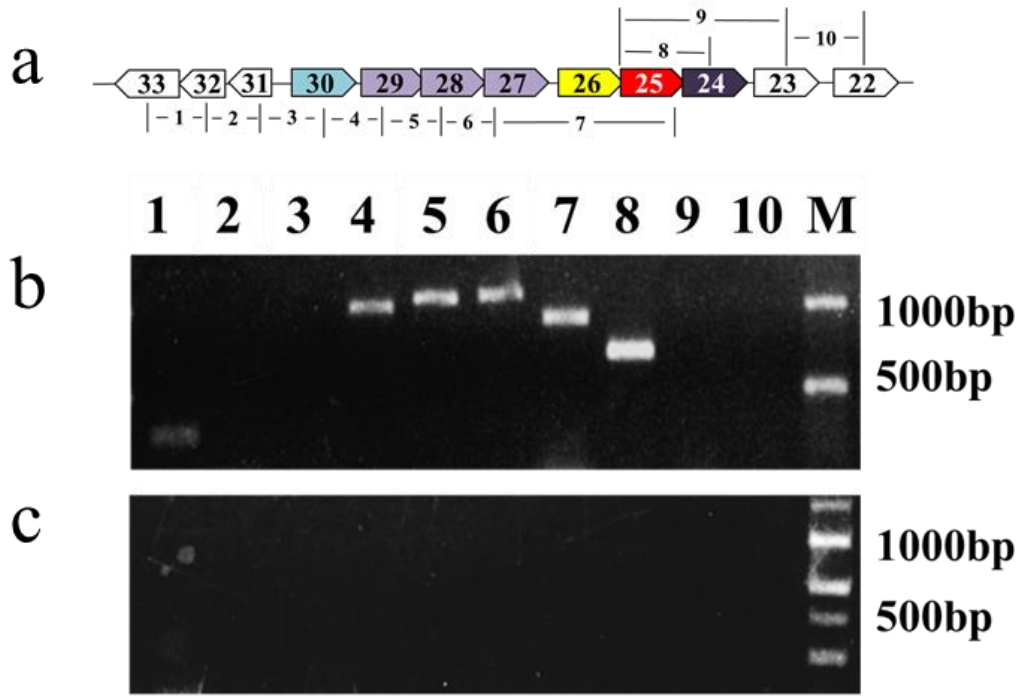

Figure 5-3-2 Identification of an operon including TTC0125-TTC0126 by RT-PCR.

(a) Arrows indicate the genetic organization of ORFs TTC0126 (26, VapB) and TTC0125 (25, VapC), as well as the upstream genes TTC0133 (33, annotated to a N-acyl-L-amino acid amidohydrolase), TTC0132 (32, annotated as a probable transcriptional regulator), TTC0131 (31, annotated to an IclR family transcriptional regulator), TTC0130 (30, annotated to a malate synthase), TTC0129 (29, annotated to (S)-2-hydroxy-acid oxidase subunit glcF), TTC0128 (28, annotated to (S)-2-hydroxy-acid oxidase subunit glcE), TTC0127 (27, annotated to (S)-2-hydroxy-acid oxidase subunit glcF), and the downstream genes TTC0124 (24, annotated to a glycerate dehydrogenase/hydroxypyruvate reductase), TTC0123 (23, annotated to a coproporphyrinogen oxidase), TTC0122 (22, annotated to a hypothetical cytosolic protein). Colored arrows indicated the operon genes of TTC0130~TTC0124. Locations and the lengths of the expected amplified fragments are shown with numbers.

Conventional RT-PCR analysis of operon using cDNA **(b)** as a template or total RNA without reverse transcription **(c)** as negative control. The reactions amplifying TTC0133-TTC0132 (lane 1), TTC0132-TTC0131 (lane 2), TTC0131-TTC0130 (lane 3), TTC0130-TTC0129 (lane 4), TTC0129-TTC0128 (lane 5), TTC0128-TTC0127 (lane 6), TTC0127-TTC0125 (lane 7), TTC0125-TTC0124 (lane 8), TTC0125-TTC0123 (lane 9), and TTC0123-TTC0122 (lane 10) were conducted. Molecular weight markers were shown on lane 11.

Section IV - Discussion

TTC0125-TTC0126 locus is a VapBC belonging to type II toxin-antitoxin system. As reported in upper chapter, *in vitro* analysis of TTC0125-TTC0126 locus showed that TTC0125 has a ribonuclease activity to free RNA and decay mRNA to inhibit cell growth.

Recent evidence indicates that TA loci function to modulate the global levels of translation and replication during exposure to some stresses, like antibiotics, to trigger cell persistence. Maisonneuve et al. (2013) firstly showed that only rare cells produced from wild-type of *E. coli* are multidrug tolerant, and they are able to resuscitate.

To discuss the physiological role of TTC0125-TTC0126, I firstly did a stress response assay on plate, to identify whether TTC0125-TTC0126 locus trigger phenotypic changes for stress response. For this experiment, two disruption mutant strains ΔTTC0125 and ΔTTC0125-TTC126 were generated. And for confirming the appropriate concentration of stress reagents, MIC of antibiotic was identified in advance. I cultured these disruption mutant and wild-type strains under kanamycin, ampicillin and other antibiotic stress, as well as osmotic and oxidation stress. After culturing at 65ºC for 36 h, cell growth of these strains was observed on plates (Fig. 5-3-2). Different with the hypothesis, disruption of TTC0125-TTC0126 locus showed a phenotypic change from the wild type under low concentration of kanamycin, indicating that TTC0125-TTC126 regulate stress response and affect cell growth under stress, not only affect a subpopulation to form persister cells, though TTC0125-TTC0126 locus showed no effect on other stress, including other antibiotic, oxidation or osmotic stress. So I guess that TTC0125-TTC0126 may possess a unique physiological function which is different from the reported TA systems.

Analysis of the TTC0126-TTC0125 locus in *T. thermophilus* genome revealed that it is a classic VapBC locus composed of 5′-preceding TTC0126 antitoxin gene and the following TTC0125 toxin gene (Fig. 5-3-3 a). However, TTC0125 is also overlapped by a downstream gene TTC0124, indicating that TTC0125-TTC0126 maybe not a single, bicistronic locus as a typical VapBC system, but form an operon with other genes, and this possibility was confirmed by the result of RT-PCR (Fig. 5-3-3 b). TTC0126-TTC0125 locus is actually transcribed with 4 genes upstream of TTC0126 (TTC0127, TTC0128, TTC0129 and TTC0130) and 1 gene downstream of TTC0125 (TTC0124) to form a 7 gene-operon.

The genes included in the operon are annotated to be metabolic enzymes. TTC0127, TTC0128 and TTC0129 are annotated as subunits of a (S)-2-hydroxy-acid oxidase that oxidizes glycolate to glyoxylate, and TTC0130 is annotated to be a malate synthase to generate malate from glyoxylate, involved in glyoxylate cycle.

The glyoxylate cycle is an anaplerotic pathway of the tricarboxylic acid (TCA) cycle, including two unique enzymes, isocitrate lyase (ICL) synthesizing glyoxylate, and MS synthesizing malate. Recent studies about these two enzymes showed that they are important in pathogenic bacteria for survival at the time of their infection (Dunn et al. 2009). Inhibition of ICL of *B. cenocepacia* biofilms reduced the persister fraction at approx. 10-fold when the biofilms were subsequently treated with tobramycin, as surviving persister cells downregulate the TCA cycle to avoid production of reactive oxygen species (ROS) and at the same time activate the glyoxylate shunt (Van Acker et al. 2013). And as Dwyer et al (2014) reported, downstream of their target-specific interactions, bactericidal antibiotics induce complex redox alterations that result in cellular damage and death, demonstrating that ROS has a key role in antibiotic stress.

So, there is a possibility that the kanamycin-tolerant phenotype of the TTC0125-TTC0126 disruption mutants is triggered by the function of compounds within glyoxylate cycle, which are related to the operon genes. However, the detailed relation of TTC0125-TTC0126 locus and operon genes is remain unknown.

The results in this chapter offered a clue that how toxin-antitoxin system triggers stress-tolerance and firstly focused on their function specific to other metabolic genes.

CONCLUSION

4 VapBC and 3 HicBA toxin-antitoxin loci were predicted in the genome of *T. thermophilus* HB27. BLAST analysis and phylogenetic tree based on amino acid sequences of the 7 toxins with typical VapC and HicA toxins confirming that TTC0113, TTC0125, TTC1207, and TTC1804 are VapCs, and TTC1395, TTC1549, TTC1705 are HicAs.

In chapter II, I analyzed toxic function of the 7 TA loci. Toxin genes were expressed with or without their cognate antitoxin genes in *E. coli*. Fig. 2-3-2 showed that expression of one VapC (TTC0125) and two HicA (TTC1395, TTC1549) genes strictly inhibited cell growth, and the growth-inhibitory effects of the former three toxin genes were more evident at 43 °C than at 37 °C, indicated that these three loci function as classic TA systems in *T. thermophilus*. However, I cannot exclude the possibility that these four toxins may also possess toxin activities at higher temperatures, i.e. the growth temperature of *T. thermophilus*.

In chapter III, I focused on the TTC0125-TTC0126 locus, the only functional VapBC TA locus in *T. thermophilus*. In this chapter, I described biochemical analyses to identify the enzyme activity of TTC0125 and its target intracellular molecules. Firstly, purification of TTC0125 and TTC0126 was conducted for biochemical analyses. Using the method described by Winther and Gerdes (2011), toxic TTC0125 protein could be produced in *E. coli* as a TTC0125-TTC0126 protein complex and purified to homogeniety. Secondly, I identified the enzyme activity of TTC0125 using the purificated proteins of TTC0125 and TTC0126. An RNase assay was performed using

total RNA isolated from both *E. coli* and *T. thermophilus* as substrates (Fig. 3-3-2), demonstrated that TTC0125 could degrade 16S and 23S rRNA and TTC0126, the antitoxin of TTC0125, could completely neutralize TTC0125's activity. To examine whether TTC0125 has substrate specificities or not, I checked its activity toward intact ribosomes (Fig. 3-3-3) and confirmed that TTC0125 only cleaves free RNA, but not RNA within intact ribosome. For assessment of initiator tRNA cleavage, the initiator tRNA of *E. coli* was detected by Northern blot hybridization, and showed that TTC0125 did not react with the initiator tRNA. On the other hand, TTC0125 degrades *in vitro*-transcribed mRNA of *E. coli* gene (*tetR*) in the same manner as total RNA (Fig. 3-3-2). Thus I concluded that TTC0125 does not have any substrate and sequence specificity, rather it degrades free RNA. Moreover, to obtain some insights into *in vivo* molecular function of TTC0125, an *in vitro*-translation inhibition assay was conducted, using a PURERex kit. The result shown in Fig. 3-3-4 indicated that TTC0125 TTC0125 inhibits translation by degrading mRNA, but not ribosome.

In chapter IV, I conducted site-directed mutagenesis to identify catalytically-important residues of TTC0125. An amino acid sequence alignment of TTC0125 with some "reviewed" VapCs in the Uniprot database (Fig. 4-3-1), indicates that some residues, including the putative catalytic residues in PIN proteins, D4, E40 and D99 in TTC0125 numbering, are conserved in all the VapCs. Also, some other residues are conserved in several, but not all, VapCs. I have selected such residues, including the catalytic residues, and introduced single amino acid substitutions to Ala or Asp. Growth inhibition assay of 14 mutants of TTC0125 indicated that E23A, T72A, L105D, and V108D did not lose their toxic activity when expressed them in *E.coli*, suggesting that

these residues are not required for its activity. The F71A mutant showed a weaker growth inhibition, suggesting that this residue may be required for this activity to some extent. In contrast, the D4A, E40A, A76D, G94D, G98D, D99A, S102D, D119A, and D124A 364 mutants, including the mutants of the putative catalytic residues, had almost no effect on cell growth, demonstrating the importance of these residues for its toxin activity. By RNase assay of purified mutant proteins, I confirmed that nine residues conserved in TTC0125 are important for the activity of enzyme.They are D4, E40, A76, G94, G98, D99, S102, D119 and D124. Among them, the three tightly conserved ones, D4, E40, and D99, are confirmed to be catalytic residues, as reported in other VapC; and A76, G94, G98, S102, D119 and D124 are confirmed to be catalytic residues experimentally by this study at first.

TTC0125-TTC0126 locus is a VapBC belonging to type II toxin-antitoxin system. As reported in upper chapter, *in vitro* analysis of TTC0125-TTC0126 locus showed that TTC0125 has a ribonuclease activity to free RNA and decay mRNA to inhibit cell growth. To discuss the physiological role of TTC0125-TTC0126, I firstly did a stress response assay on plate, to identify whether TTC0125-TTC0126 locus trigger phenotypic changes for stress response. For this experiment, two disruption mutant strains ΔTTC0125 and ΔTTC0125-TTC126 were generated. And for confirming the appropriate concentration of stress reagents, MIC of antibiotic was identified in advance. I cultured these disruption mutant and wild-type strains under kanamycin, ampicillin and other antibiotic stress, as well as osmotic and oxidation stress. After culturing at 65ºC for 36 h, cell growth of these strains was observed on plates (Fig. 5-3-2). Different with the hypothesis, disruption of TTC0125-TTC0126 locus showed a phenotypic

change from the wild type under low concentration of kanamycin, indicating that TTC0125-TTC126 regulate stress response and affect cell growth under stress, not only affect a subpopulation to form persister cells, though TTC0125-TTC0126 locus showed no effect on other stress, including other antibiotic, oxidation or osmotic stress. So I guess that TTC0125-TTC0126 may possess a unique physiological function which is different from the reported TA systems.

Analysis of the TTC0126-TTC0125 locus in *T. thermophilus* genome revealed that it is a classic VapBC locus composed of 5′-preceding TTC0126 antitoxin gene and the following TTC0125 toxin gene (Fig. 5-3-3 a). However, TTC0125 is also overlapped by a downstream gene TTC0124, indicating that TTC0125-TTC0126 maybe not a single, bicistronic locus as a typical VapBC system, but form an operon with other genes, and this possibility was confirmed by the result of RT-PCR (Fig. 5-3-3 b). TTC0126-TTC0125 locus is actually transcribed with 4 genes upstream of TTC0126 (TTC0127, TTC0128, TTC0129 and TTC0130) and 1 gene downstream of TTC0125 (TTC0124) to form a 7 gene-operon.

The genes included in the operon are annotated to be metabolic enzymes. TTC0127, TTC0128 and TTC0129 are annotated as subunits of a (S)-2-hydroxy-acid oxidase (oxidizes glycolate to glyoxylate), and TTC0130 is annotated to be a malate synthase to generate malate from glyoxylate, involved in glyoxylate cycle. There is a possibility that the kanamycin-tolerant phenotype of the TTC0125-TTC0126 disruption mutants is triggered by the function of compounds within glyoxylate cycle, which are related to the operon genes. However, the detailed relation of TTC0125-TTC0126 locus and operon genes is remain unknown. The results in this chapter offered a clue that how

toxin-antitoxin system triggers stress-tolerance and firstly focused on their function specific to other metabolic genes.

In conclusion, I characterized seven putative TA loci in *T. thermophilus*, and found that the three loci, TTC0125-TTC0126, TTC1395-TTC1396, and TTC1705-397 TTC1706, function as a TA module, indicated by the *E. coli* growth-inhibition assay. Biochemical analysis indicated that TTC0125 catalyzes degradation of RNA and inhibits translation by degrading free mRNA, and TTC0126 inhibits its activity as the antitoxin. Nine catalytically-important residues in TTC0125, including the three putative catalytic residues, were identified, most of which are located near the catalytic center of the three-dimensional model. Most vapBC loci in microorganisms consist of a bicystronic operon but the TTC0125-TTC0126 locus is included in a gene cluster encoding metabolic enzymes related to the glyoxylate cycle. It is possible that the physiological function of TTC0125-TTC0126 is related to this cycle. It is the first report that indicated a TA locus is transcribed with a metabolic gene-operon, and also suggested the impossibility of interaction between TA locus and metabolic genes.

AKNOWLEDGEMENTS

This research work owns great debts to Professor Dr. Akira Nakamura, for the conception of this study. I would like to express here my sincere gratitude for the advice, guidance and support given among all those years.

I would like to acknowledge Professor Dr. Takayuki Hoshino, Professor Dr. Naoki Takaya and Associate Professor Dr. Beiwen Ying, for the precious suggestions in the execution of experiments and guidance.

I also would like to acknowledge Associate Professor Dr. Shengmin Zhou, for his help for the experiments.

I acknowledge the Ministry of Education, Culture, Science and Technology of Japan for the financial support, and giving me the unique opportunity to study in Japan, making an old dream come true.

I express my warm thanks to the fellows of the Environmental Molecular Biology Laboratory, for the friendship and all good moments together.

A very special acknowledgement goes to my husband and child, whom endured long-time separation but still loved and supported me during the critical moments of these years.

Lastly, heartily thanks are presented to my beloved parents, Jing Fan and Jianhua Cui for their permanent encouragement and support. Every step that I took in

life was a consequence of your unconditional love, the conclusion of this doctor degree is another small step, of a long walking that I made all the time together with you all, no matter how far apart we are.

Tsukuba, January 2017

Yuqi Fan

REFERENCES

Akanuma S, Nakajima Y, Yokobori S, Kimura M, Nemoto N, Mase T, Miyazono K, Tanokura M, Yamagishi A (2013) Experimental evidence for the thermophilicity of ancestral life. Proc Natl Acad Sci 110: 11067–110672.

Arcus VL, Bäckbro K, Roos A, Daniel EL, Baker EN (2004) Distant structural homology leads to the functional characterization of an archaeal PIN domain as an exonuclease. The Journal of Biological Chemistry 279: 16471–16478.

Arcus VL, Mckenzie JL, Robson J, Cook GM (2011) The PIN-domain ribonucleases and the prokaryotic VapBC toxin-antitoxin array. Protein Engineering, Design and Selection 24: 33–40.

Bertram R, Schuster CF (2014) Post-transcriptional regulation of gene expression in bacterial pathogens by toxin-antitoxin systems. Frontiers in Cellular and Infection Microbiology 4:6.

Brasier MD, Green OR, Jephcoat AP, Kleppe AK, Van Kranendonk MJ, Lindsay JF, Steele A, Grassineau NV (2002). Questioning the evidence for Earth's oldest fossils. Nature 416: 76–81.

Bunker RD, McKenzie JL, Baker EN, Arcus VL (2008) Crystal structure of PAEO151 from *Pyrobaculum aerophilum*, a PIN-domain (VapC) protein from a toxin-antitoxin operon. Proteins 72:510–518.

Butt A, Higman V, Williams C, Crump MP, Hemsley CM, Harmer N, Titball RW (2014) The HicA toxin from *Burkholderia pseudomallei* has a role in persister cell formation. The Biochemical Journal 459: 333–44.

Christensen SK, Gerdes K (2003) RelE toxins from Bacteria and Archaea cleave mRNAs on translating ribosomes, which are rescued by tmRNA. Molecular

Microbiology 48: 1389–1400.

Daines DA, Wu MH, Yuan SY (2007) VapC-1 of nontypeable *Haemophilus influenzae* is a ribonuclease. Journal of Bacteriology 189: 5041–8.

Das U, Pogenberg V, Subhramanyam UK, Wilmanns M, Gourinath S, Srinivasan A (2014) Crystal structure of the VapBc-15 complex from *Mycobacterium tuberculosis* reveals a two-metal ion dependent pin-domain ribonuclease and a variable mode of toxin-antitoxin assembly. Journal of Structural Biology 188:249–258.

Dienemann C, Bøggild A, Winther KS, Gerdes K, Brodersen DE (2011) Crystal structure of the VapBC toxin–antitoxin complex from *Shigella flexneri* reveals a hetero-octameric DNA-binding assembly. Journal of Molecular Biology journal 414:713-722.

Fauvart M, De Groote VN, Michiels J (2011) Role of persister cells in chronic infections: Clinical relevance and perspectives on anti-persister therapies. Journal of Medical Microbiology 60: 699–709.

Finn RD, Mistry J, Tate J, Coggill1 P, Heger A, Pollington JE, Gavin OL, Gunasekaran P, Ceric G, Forslund K, Holm L, Sonnhammer EL, Eddy SR, Bateman A (2010) The Pfam protein families databases. Nucleic Acids Research 38: D211-D222.

Gerdes K (2000) Toxin-antitoxin modules may regulate synthesis of macromolecules during nutritional stress. Journal of Bacteriology 182: 561–572.

Gerdes K, Christensen SK, Løbner-Olesen A (2005) Prokaryotic toxin-antitoxin stress response loci. Nature Reviews. Microbiology 3: 371–82.

Germain E, Castro-Roa D, Zenkin N, Gerdes K (2013) Molecular mechanism of bacterial persistence by HipA. Molecular Cell 52: 248–54.

Griffiths E, Gupta RS (2007) Identification of signature proteins that are distinctive of the *Deinococcus-Thermus* phylum. International Microbiology 10: 201–208.

Grønlund H, Gerdes K (1999) Toxin-antitoxin systems homologous with relBE of *Escherichia coli* plasmid P307 are ubiquitous in prokaryotes. Journal of Molecular Biology 285: 1401–15.

Henne A, Brüggemann H, Raasch C, Wiezer A, Hartsch T, Liesegang H, Fritz HJ (2004) The genome sequence of the extreme thermophile *Thermus thermophilus*. Nature Biotechnology 22: 547–553.

Jørgensen MG, Pandey DP, Jaskolska M, Gerdes K (2009) HicA of *Escherichia coli* defines a novel family of translation-independent mRNA interferases in bacteria and archaea. Journal of Bacteriology 191: 1191–9.

Kelly LA, Mezulis S, Yates C, Wass M, Sternberg M (2015) The Phyre2 web portal for protein modelling, prediction, and analysis. Nature Protocols 10: 845–858.

Koyama Y, Hoshino T, Tomizuka N, Furukawa K (1986) Genetic transformation of the extreme thermophile *Thermus thermophilus* and of other Thermus spp. J Bacteriol 166: 338–340.

Laemmli UK (1970) Cleavage of structural proteins during the assembly of the head of bacteriophage T4. Nature 227: 680–685.

Lee IG, Lee SJ, Chae S, Lee KY, Kim JH, Lee BJ (2015) Structural and functional studies of the *Mycobacterium tuberculosis* VapBC30 toxin-antitoxin system: implications for the design of novel antimicrobial peptides. Nucleic Acids Research 43: 7624–37.

Li G, Shen M, Lu S, Le S, Tan Y, Wang J, Li, M (2016) Identification and characterization of the HicAB toxin-antitoxin system in the opportunistic pathogen *Pseudomonas aeruginosa*. Toxins 8: 1–12.

Lutz R, Bujard H (1997) Independent and tight regulation of transcriptional units in *Escherichia coli* via the LacR/O, the TetR/O and AraC/I1-I2 regulatory elements. Nucleic Acids Research 25: 1203–1210.

Maezato Y, Daugherty A, Dana K, Soo E, Cooper C, Tachdjian S, Blum P (2011) VapC6, a ribonucleolytic toxin regulates thermophilicity in the crenarchaeote *Sulfolobus solfataricus*. RNA 17: 1381–92.

Maisonneuve E, Castro-Camargo M, Gerdes K (2013) (p)ppGpp controls bacterial persistence by stochastic induction of toxin-antitoxin activity. Cell 154: 1140–50.

Maisonneuve E, Gerdes K (2014) Molecular mechanisms underlying bacterial persisters. Cell 157: 539–48.

Makarova KS, Grishin NV, Koonin EV (2006) The HicAB cassette, a putative novel, RNA-targeting toxin-antitoxin system in archaea and bacteria. Bioinformatics 22: 2581–4.

Makarova KS, Wolf YI, Koonin EV (2009) Comprehensive comparative-genomic analysis of type 2 toxin-antitoxin systems and related mobile stress response systems in prokaryotes. Biology Direct 4: 19.

McKenzie JL, Duyvestyn JM, Smith T, Bendak K, Mackay J, Cursons R, Arcus VL (2012) Determination of ribonuclease sequence-specificity using Pentaprobes and mass spectrometry. RNA 18: 1267–78.

Min AB, Miallau L, Sawaya MR, Habel J, Cascio D, Eisenberg D (2012) The crystal structure of the Rv0301-Rv0300 VapBC-3 toxin-antitoxin complex from *M. tuberculosis* reveals a Mg2+ ion in the active site and a putative RNA-binding site. Protein Science 21: 1754–1767.

Notredame C, Higgins DG, Heringa J (2000) T-coffee: a novel method for fast and accurate multiple sequence alignment. Journal of Molecular Biology 302: 205–

217.

Omelchenko MV, Wolf YI, Gaidamakova EK, Matrosova VY, Vasilenko A, Zhai M, Makarova KS (2005) Comparative genomics of *Thermus thermophilus* and *Deinococcus radiodurans*: divergent routes of adaptation to thermophily and radiation resistance. BMC Evolutionary Biology, 5: 57.

Oshima T, Imahori K (1974) Physiochemical properties of deoxyribonucleic acid from an extreme thermophile. Journal of Biochemistry 75: 179–83.

Pace NR (1991) Origin of life-facing up to the physical setting. Cell 65: 531–533.

Page R, Peti W (2016) Toxin-antitoxin systems in bacterial growth arrest and persistence. Nat Chem Biol 12: 208–214.

Pongs O, Bald R, Erdmann VA (1973) Identification of chloramphenicol-binding protein in *Escherichia coli* ribosomes by affinity labeling. PNAS 70: 2229–33.

Ramage HR, Connolly LE, Cox JS (2009) Comprehensive Functional Analysis of *Mycobacterium tuberculosis* Toxin-Antitoxin Systems: Implications for Pathogenesis, Stress Responses, and Evolution. PLoS Genetics 5: e1000767.

Rastogi G, Bhalla A, Adhikari A, Bischoff KM, Hughes SR, Christopher LP, Sani RK (2010) Characterization of thermostable cellulases produced by *Bacillus* and *Geobacillus* strains. Bioresource Technology 101: 8798–8806.

Ruiz-Echevarría MJ, de Torrontegui G, Giménez-Gallego G, Díaz-Orejas R (1991) Structural and functional comparison between the stability systems ParD of plasmid R1 and Ccd of plasmid F. Molecular and General Genetics 225: 355–362.

Shao Y, Harrison EM, Bi D, Tai C, He X, Ou HY, Deng Z (2011) TADB: A web-based resource for Type 2 toxin-antitoxin loci in bacteria and archaea. Nucleic Acids Research 39: 606–611.

Sharp JD, Cruz JW, Raman S, Inouye M, Husson RN, Woychik NA (2012) Growth and translation inhibition through sequence-specific RNA binding by *Mycobacterium tuberculosis* VapC toxin. Journal of Biological Chemistry 287: 12835–12847.

Shimizu Y, Inoue A, Tomari Y, Suzuki T, Yokogawa T, Nishikawa K, Ueda T (2001) Cell-free translation reconstituted with purified components. Nature Biotechnology, 19: 751–5.

Stetter KO (2006) Hyperthermophiles in the history of life. Philosophical Transactions B 361:1837–1843.

Takayama G, Kosuge T, Maseda H, Nakamura A, Hoshino T (2004) Nucleotide sequence of the cryptic plasmid pTT8 from *Thermus thermophilus* HB8 and isolation and characterization of its high-copy-number mutant. Plasmid 51: 227–237.

Trauner A, Bennett MH, Williams HD (2011) Isolation of bacterial ribosomes with monolith chromatography. PLoS ONE 6: e16273.

Unterholzner SJ, Poppenberger B, Rozhon W (2014) Toxin-antitoxin systems. Bioengineered 5: 1–13.

Urbieta MS, Donati ER, Chan KG, Shahar S, Sin LL, Goh KM (2015) Thermophiles in the genomic era: Biodiversity, science, and applications. Biotechnology Advances 33: 633–647.

Vesper O, Amitai S, Belitsky M, Byrgazov K, Kaberdina AC, Engelberg-Kulka H, Moll I (2011) Selective translation of leaderless mRNAs by specialized ribosomes generated by MazF in *Escherichia coli*. Cell 147: 147–157.

Wang X, Wood TK (2011) Toxin-antitoxin systems influence biofilm and persister cell formation and the general stress response. Applied and Environmental Microbiology 77: 5577–5583.

Wimberly BT, Brodersen DE, William MC, Clemons WM, Jr, Robert J. Morgan-Warren TJ, Carter AP, Vonrhein C, Hartsch T, Ramakrishnan V (2000) Structure of the 30S ribosomal subunit. Nature 327–339.

Winther KS, Brodersen DE, Brown AK, Gerdes K (2013) VapC20 of *Mycobacterium tuberculosis* cleaves the sarcin-ricin loop of 23S rRNA. Nature Communications 4:2796.

Winther KS, Gerdes K (2011) Enteric virulence associated protein VapC inhibits translation by cleavage of initiator tRNA. PNAS 108: 7403–7.

Winther K, Tree JJ, Tollervey D, Gerdes K (2016) VapCs of *Mycobacterium tuberculosis* cleave RNAs essential for translation. Nucleic Acids Research 44: 9860-9871.

Woese CR (1987) Bacterial evolution. Microbiological Reviews 51: 221–71.

Zhu L, Sharp JD, Kobayashi H, Woychik NA, Inouye M (2010) Noncognate *Mycobacterium tuberculosis* toxin-antitoxins can physically and functionally interact. The Journal of Biological Chemistry, 285: 39732–8.